ABITEC
AN ABF INGREDIENTS COMPANY

Technical Data Sheet

10/27/2020

CAPMUL® MCM

Ingredients: Caprylic/capric mono- & diglycerides
Chemical Name: Glyceryl caprylate/caprate
Synonyms: Glycerol monocaprylocaprate; Glycerides C8-10 mono-, di-, tri-; Medium chain mono- & diglycerides; Glyceryl mono- & dicaprylo/caprate; Mono-diglycerides of caprylic/capric acid

Description

Capmul MCM is a mono-diglyceride of medium chain fatty acids (mainly caprylic and capric). It is an excellent solvent for many organic compounds, including steroids. It is also a useful emulsifier for water-oil (w/o) systems.

Specifications

Specification	Limit	Reference Method
Color, Lovibond (Red)	≤4.0 R	[1]AOCS Cc13j-97
Acid value (mg KOH/g)	≤2.5	AOCS Cd 3d-63
Iodine Value (cg I_2/g)	≤2.0	AOCS Cd 1c-85
Free Glycerol (%)	≤2.5	AOCS Ca14-56
Moisture, Karl Fischer (%)	≤0.5	AOCS Ca 2e-84
Alpha Monocaprylocaprate (as oleate) (%)	≥48 ≥80	AOCS Cd 11-57

[1]AOCS: American Oil Chemists' Society

Typical Properties

Property	Description
Appearance @ 25°C	Colorless or slightly yellow oily liquid or soft mass
Specific Gravity	0.97 – 1.02

Nutritional Applications

- Bioavailability enhancer
- Solubilizer
- Emulsifier / co-emulsifier
- Carrier (vehicle)
- Penetration enhancer (dermatological applications)

Personal Care Applications

- Water / oil emulsifier
- Recommended for creams, lotions, ointments, and lipsticks

Recommended Storage and Handling

- Store in tight, light-resistant containers
- Store in a dry location at ambient temperature
- Retest/requalify 20 months after date of manufacture
- Contents of package must be heated slightly with agitation to ensure uniformity prior to use (maximum of 6 heat cycles), details upon request.

Regulatory

- Generally recognized as safe (GRAS) when used according to 21 CFR § 184.1505.

Standard Packaging

- Tank wagon
- 425 lb (192.8 kg) drum
- 50 lb (22.7 kg) HDPE jerrican

501 West First Avenue, Columbus, OH, USA 43215 | Toll Free: 800-555-1255 | info@abiteccorp.com | www.abiteccorp.com

European Journal of Pharmaceutics and Biopharmaceutics 96 (2015) 363–379

Contents lists available at ScienceDirect

European Journal of Pharmaceutics and Biopharmaceutics

journal homepage: www.elsevier.com/locate/ejpb

Research Paper

Intranasal microemulsion for targeted nose to brain delivery in neurocysticercosis: Role of docosahexaenoic acid

Rajshree L. Shinde [a], Gopal P. Bharkad [b], Padma V. Devarajan [a,*]

[a] Department of Pharmaceutical Sciences and Technology, Institute of Chemical Technology, N.P. Marg, Matunga (E), Mumbai, Maharashtra, India
[b] Department of Veterinary Parasitology, Bombay Veterinary College, Parel, Mumbai, Maharashtra, India

ARTICLE INFO

Article history:
Received 26 April 2015
Revised 12 August 2015
Accepted in revised form 18 August 2015
Available online 28 August 2015

Chemical compounds studied in this article:
Albendazole sulfoxide (PubChem CID: 83969)
Curcumin (PubChem CID: 969516)
Docosahexaenoic acid (PubChem CID: 175542)
Capmul MCM (PubChem CID: 3033877)
Tween 80 (PubChem CID: 5281955)
Ethanol (PubChem CID: 702)
Propylene glycol (PubChem CID: 1030)
N,N-dimethylacetamide (PubChem CID: 31374)
Acetonitrile (PubChem CID: 6342)

Keywords:
Intranasal microemulsions
Docosahexaenoic acid (DHA)
Neurocysticercosis
Albendazole sulfoxide
Curcumin
Nose to brain delivery
Ex vivo permeation
Drug targeting efficiency (DTE)
Direct nose to brain transport (DTP)
Taenia solium cyst.

ABSTRACT

Intranasal Microemulsions (MEs) for nose to brain delivery of a novel combination of Albendazole sulfoxide (ABZ-SO) and Curcumin (CUR) for Neurocysticercosis (NCC), a brain infection are reported. MEs prepared by simple solution exhibited a globule size <20 nm, negative zeta potential and good stability. The docosahexaenoic acid (DHA) ME revealed high and rapid ex vivo permeation of drugs through sheep nasal mucosa. Intranasal DHA ME resulted in high brain concentrations and 10.76 (ABZ-SO) and 3.24 (CUR) fold enhancement in brain area-under-the-curve (AUC) compared to intravenous DHA MEs at the same dose. Direct nose to brain transport (DTP) of >95% was seen for both drugs. High drug targeting efficiency (DTE) to the brain compared to Capmul ME and drug solution ($P < 0.05$) suggested the role of DHA in aiding nose to brain delivery. Histopathology study confirmed no significant changes. High efficacy of ABZ-SO: CUR (100:10 ng/mL) DHA ME in vitro on *Taenia solium* cysts was confirmed by complete ALP inhibition and disintegration of cysts at 96 h. Considering that the brain concentration at 24 h was 1400 ± 160.1 ng/g (ABZ-SO) and 120 ± 35.2 ng/g (CUR), the in vitro efficacy seen at a 10 fold lower concentration of the drugs strongly supports the assumption of clinical efficacy. The intranasal DHA ME is a promising delivery system for targeted nose to brain delivery.

Abbreviations: ABZ, albendazole; ABZ-SO, Albendazole sulfoxide; ACN, acetonitrile; ALP, alkaline phosphatase; ANOVA, analysis of variance; AUC, area-under-the-curve; BBB, blood brain barrier; C_{max}, maximum concentration; CUR, Curcumin; CYPs, cytochrome P450; DHA, docosahexaenoic acid; DTE, drug targeting efficiency; DTP, nose to brain direct transport; FMO, flavin-containing mono-oxygenase; HPLC, high performance liquid chromatography; ICH guidelines, International Conference on Harmonisation guidelines; i.n., intranasal; i.v., intravenous; LOD, limit of detection; LOQ, limit of quantification; NCC, Neurocysticercosis; NEs, nanoemulsions; MEs, Microemulsions; PBS, phosphate buffer saline; PDI, polydispersity index; PEG 400, polyethylene glycol 400; PUFA, polyunsaturated fatty acid; RH, relative humidity; SANS, small-angle neutron scattering; J_{ss}, steady state flux; $t_{1/2}$, half-life; *T. solium*, *Taenia solium*; TEM, transmission electron microscopy; t_{max}, time to reach C_{max}.

* Corresponding author at: Department of Pharmaceutical Sciences and Technology, Institute of Chemical Technology, N.P. Marg, Matunga, Mumbai 400019, Maharashtra, India. Tel.: +91 2233612201; fax: +91 2233611020.
E-mail address: pvdevarajan@gmail.com (P.V. Devarajan).

http://dx.doi.org/10.1016/j.ejpb.2015.08.008
0939-6411/

1. Introduction

Targeted nose to brain delivery is a proven strategy to circumvent the blood brain barrier (BBB) and hence achieve high drug concentration in the brain [1,2]. Number of drugs have been targeted to the brain for various therapeutic indications including cancer [3], schizophrenia [4], Alzheimer's [5], Parkinson's [6], migraine [7], and even infections such as encephalitis and meningitis [8]. Nevertheless an important brain infection that has been ignored for targeted drug delivery to the brain is Neurocysticercosis (NCC).

NCC, a contagious zoonotic and orphan disease, spreads rapidly through contaminated pork [9,10]. Caused by the cystic larval stage of the parasite *Taenia solium* (tapeworm), NCC manifests as adult acquired seizures and if untreated could also be fatal [11,12]. Standard therapy for NCC is a combination of albendazole (ABZ) and corticosteroids [9]. ABZ, however exhibits poor oral bioavailability with limited concentration in the brain due to the insurmountable blood brain barrier (BBB) [13]. Targeted nose to brain delivery provides a promising strategy to enhance drug concentration in the brain and thereby improved cure rates of NCC.

Microemulsions (MEs) and nanoemulsions (NEs) provide definite advantages including high loading of hydrophobic and hydrophilic drugs, feasibility of sterilization and the possibility of targeted and controlled drug delivery and are hence widely investigated for intranasal delivery [14,15]. Intranasal administration of mucoadhesive MEs of sumatriptan [16], clonazepam [17] and tacrine [5] revealed higher brain/blood ratios compared to intravenous (i.v.) suggesting effective brain targeting. A high drug targeting efficiency (%DTE) and nose to brain direct transport (% DTP) were seen with NEs of olanzapine [18], risperidone [19] and zolmitriptan ([20]. Direct nose to brain transport of nimodipine ME confirmed that a fraction of nimodipine could be transported directly into the brain following nasal delivery [21].

NE components often play a crucial role in enabling delivery across the BBB [22]. MEs comprising long chain triglycerides exhibit prolonged circulation half-life and hence greater brain accumulation [3,15,22]. Flax-seed oil, enabled significantly high and comparable brain targeting of saquinavir following intravenous and oral administration in comparison with safflower oil although both comprised polyunsaturated fatty acid (PUFA). Nevertheless flax-seed oil is naturally more PUFA enriched than safflower oil. The slow metabolism and elimination of PUFA oils also favoured sustained drug concentration in the brain [22]. PUFA, specifically docosahexaenoic acid [DHA, 22:6(n-3)] has natural transporters across the BBB and furthermore DHA enabled enhanced permeation across sheep nasal mucosa ex vivo. DHA being an important nutrient for brain health could provide additional advantage [23]. We therefore designed MEs containing DHA in the oil phase for intranasal delivery. Although ABZ is the drug of choice for NCC we selected ABZ-SO the active metabolite of ABZ, as the active.

ABZ a prodrug is metabolized to the active metabolite albendazole sulfoxide (ABZ-SO) by cytochrome P450 (CYPs) and the flavin-containing mono-oxygenase (FMO) system predominantly in the liver and intestine [11,24]. The limited presence of CYPs in the nasal mucosa precluded the intranasal administration of ABZ dictating the use of the metabolite ABZ-SO. The long term therapy associated with NCC and the related side effects of the co-administered corticosteroids prompted us to replace the same with a safe and natural anti-inflammatory agent Curcumin (CUR) [25].

Our study therefore presents a novel combination of ABZ-SO and CUR in a ME formulation comprising a PUFA rich oil (DHA rich oil) with the objective of targeted and sustained brain delivery following intranasal administration.

The enhancement in brain concentrations following nasal administration was compared with the same formulations administered intravenously. The specific objective of study was to evaluate the role of the DHA rich oil in the ME on enhanced brain targeting.

An in vitro efficacy study of the MEs on *Taenia solium* (*T. solium*) cysts (Cysticercus cellulosae) was also undertaken as an indicator of possible efficacy in vivo. The decrease in cyst size and alkaline phosphatase (ALP) levels was retained as parameters of in vitro efficacy study.

2. Materials and methods

2.1. Materials

Albendazole sulphoxide and curcumin were obtained as a gift sample from SeQuent Scientific Limited (India) (assay 99.9%) and Konark herbals and Healthcare, India (assay 99.9%) respectively. DHA rich oil [INCHROMEGA DHA 500 TG SR, Croda Chemicals (India) Private Limited] and Capmul MCM (Abitec Corporation Ltd., India) were obtained as gift samples. Tween 80, ethanol, propylene glycol, N,N-dimethylacetamide, methanol, and acetonitrile were procured from Merck India Pvt. Ltd. RPMI 1640 medium supplemented with L-glutamine (2 mM), HEPES buffer (25 mM; Gibco-Invitrogen), penicillin (10,000 U/mL), streptomycin (10 mg/mL), amphotericin B (0.25 mg/mL) and 10% foetal bovine serum; all were purchased from Gibco-Invitrogen. The in vitro assays were carried out in cell culture 12 well plates (Corning, USA). All other chemicals were of analytical reagent grade or HPLC grade.

2.2. Solubility study

The solubility of drugs in the ME components was determined by adding excess of drug (ABZ-SO/CUR) to 1 mL each of selected oils, surfactants and co-surfactants in Eppendorf tubes (1.5 mL). Solubility in combination with oil was also evaluated. The Eppendorf tubes were maintained at 37 ± 1 °C in a shaker water bath for 48 h to attain equilibrium. The equilibrated samples were centrifuged at 10,000*g* for 15 min and the supernatant was analyzed by UV spectrophotometry at λ_{max} 290 nm (ABZ-SO) and 425 nm (CUR).

2.3. Pseudoternary phase diagram

Selection of appropriate components for the formation of o/w ME was based on pseudoternary phase diagrams. The surfactant and cosurfactant (CoS) selected were tween 80 and ethanol respectively. The oils employed in the present study were DHA, Capmul MCM and their combination. Pseudoternary phase diagrams of oil, surfactant, (CoS), and water were constructed using the oil titration method to obtain the components and their concentration ranges that can result in large existence area of ME. The surfactant was blended with CoS (S_{mix}) in fixed weight ratios (1:1, 2:1 and 3:1). Water and S_{mix} were mixed at room temperature (25 °C) in the ratios 9:1, 8:2, 7:3, 6:4, 5:5, 4:6, 3:7, 2:8, and 1:9 (w/w). Oil was added dropwise to each water–S_{mix} mixture and vortexed. After equilibrium, the samples were visually checked using optical polarizer and determined as being clear ME or emulsions, or gels, and the phase diagrams plotted.

2.4. Drug loaded microemulsions

The ME composition comprised 60% tween 80:ethanol (3:1) and 30% water by weight. The oil concentration was maintained at 10% and comprised either DHA rich oil:Capmul MCM (1:1) or Capmul MCM. MEs comprising DHA rich oil:Capmul MCM (1:1) in the oil phase are referred to as DHA ME while those with Capmul MCM

as oil are referred to as Capmul ME. ABZ-SO (1 mg/mL) and CUR (5 mg/mL) were added to the blank ME (1 mL) in Eppendorf tubes (1.5 mL) and vortexed on a cyclomixer. MEs comprising ABZ-SO 1 mg/mL and CUR 5 mg/mL in combination were finalized. DHA ME comprising ABZ-SO 1 mg/mL and CUR 1 mg/mL was prepared separately for in vitro study.

2.5. Characterization

2.5.1. Drug content

Drug loaded MEs in Eppendorf tubes were centrifuged at 10,000*g* for 15 min and the supernatant suitably diluted with methanol was monitored for drug content by HPLC at λ_{max} 290 nm (ABZ-SO) and 425 nm (CUR).

2.5.2. Globule size and zeta potential measurement

The average particle size, polydispersity index [PDI] and zeta potential of MEs were determined using Zetasizer [ZS 90, Malvern, UK] at 25 °C after appropriate dilution with double distilled water (1:50) [26].

2.5.3. Transmission electron microscopy (TEM)

TEM analyses were performed on a FEI Tecnai 12 BT instrument operated at 120 kV. ABZ-SO CUR DHA ME was diluted with Milli-Q water at a ratio of 1:50 and mixed by vortexing on cyclomixer. A drop of the ME was placed on a TEM grid covered by a holey carbon film, stained with 2% uranyl acetate for 10 min and blotted with filter paper to form a thin liquid film on the grid. TEM micrographs were recorded using Image Analysis software and CCD camera [27].

2.5.4. Small-angle neutron scattering (SANS)

Small-angle neutron scattering (SANS) of the ABZ-SO CUR DHA ME was recorded on a SANS diffractometer at the Bhabha Atomic Research Centre, Trombay. A beryllium oxide filtered beam of a wavelength of 5.2 Å was used. Drug loaded ME was diluted with deuterium oxide (D_2O) (ME:D_2O; 1:10 v/v) and analysed. Samples were held in a quartz sample holder of 0.5 cm thickness, at a temperature of 30 °C [28].

2.5.5. Viscosity

The viscosity at varying shear rates for MEs (100 μL) was conducted using cone and plate programmable rheometer (Physica MCR101, Germany) connected to a digital thermostatically controlled circulating water bath (Polyscience, Model 9101, USA) with spindle CP35-2-SN20784 (d = 0.147 mm) [29]. Twenty-five measurements between the shear rates of 0.01–100 s^{-1} were taken after the equipment and sample equilibrated for 5 min following loading at a constant temperature of 20 °C. Data acquisition was carried out using RHEOPLUS/32 V3.40 software version. All studies were performed in triplicate and the average value was considered.

2.5.6. Mucoadhesion test

Mucoadhesion of the formulation was measured on CT3 Texture analyser (100 g). The test was carried out in the compression mode with a trigger load of 0.5 g. An aqueous solution of 3% w/v porcine (100 μL) mucin was spread on the tissue holder of the texture analyser and allowed to dry. This served as the mucoadhesive substrate. The bottom of a closed cylindrical probe (TA-10) was dipped into the ME held on a watch glass to a form thin, continuous film on the surface of probe. The probe was lowered such that it just touched the mucoadhesive substrate, was allowed to contact for 10 s and withdrawn at a speed of 0.5 mm/s. This assembly was connected to a computer system and readings were recorded and analyzed using the TexturePro CT V1.3 Build 15 software [30]. Distilled water was used as the reference.

2.5.7. Fourier Transform Infrared (FTIR) Spectroscopy

FTIR spectra for ABZ-SO, CUR drug powder and ABZ-SO CUR DHA ME were recorded on a Perkin–Elmer FTIR spectrophotometer by the Potassium bromide (KBr) disc method from 4000 to 500 cm^{-1}. Samples were crushed to a fine powder, mulled with anhydrous potassium bromide, compressed to form a thin transparent pellet and subjected to FTIR.

2.6. Stability evaluation

2.6.1. Freeze–thaw Cycle

Four heating and cooling cycles at 40 °C and freezing (0 °C) temperature with storage at each temperature for not less than 48 hours were carried out for ABZ-SO CUR MEs.

2.6.2. Accelerated stability studies

ABZ-SO CUR MEs were filled in glass vials, stoppered and sealed and then subjected to accelerated stability studies as per International Conference on Harmonisation (ICH) guidelines at 30 °C ± 2 °C/65% relative humidity (RH) and 40 °C ± 2 °C/75% RH. In addition ABZ-SO CUR MEs were placed at ambient conditions. All samples were withdrawn at specific time intervals and evaluated for appearance, globule size and drug content by HPLC.

2.7. Haemolysis and serum stability

In vitro haemolytic potential was studied using a reported method [31]. Negative control sample was prepared by suspending red blood cell (RBC) in the 0.9% w/v NaCl solution and distilled water served as positive control. Freshly prepared ABZ-SO CUR DHA ME was mixed with 10% rat plasma in phosphate buffer saline (PBS) pH 7.4, in a ratio of 1:1 in an Eppendorf tube and incubated at 37 ± 0.5 °C. An aliquot (0.1 mL) was withdrawn at 0, 1, 2, 4, and 6 h. Serum stability was evaluated by monitoring change in globule size by Zetasizer Nano ZS (Malvern Instruments Ltd., UK) [32].

2.8. Ex vivo permeation studies

Fresh nasal mucosa was carefully removed from the nasal cavity of sheep obtained from the local slaughterhouse. Permeation study was performed using Keshary Chien diffusion cell with internal diameter of 1.6 cm and diffusion area of 2.01 cm^2. Simulated nasal fluid was used as a permeation medium (10 mL). Prior to use the membrane was equilibrated in permeation medium for 30 min, to ensure removal of all soluble components. A constant temperature (37 ± 0.5 °C) was maintained throughout the experiment using a circulating water bath. The MEs (50 μL) were added using micropipette onto the mucosal membrane. Aliquots (2 mL) were withdrawn from the receptor compartment at different time intervals (0.25, 0.5, 1, 2, 4, 6 and 8 h) using a syringe. The volume withdrawn was replenished with an equal quantity of pre-warmed permeation medium at each time point. The samples were centrifuged (10,000 rpm, 5 min) and drugs in the supernatant were quantified by HPLC. Flux data were plotted as the cumulative amount of drug diffused from nasal mucosa vs. time [33]. Permeability coefficient [P] was calculated using the following formula (1):

$$P = dQ/dt\ \mathrm{Co}A \quad (1)$$

where dQ/dt: flux or permeability rate (mg/h), Co: initial concentration in donor compartment, and A: effective surface area of nasal mucosa

2.9. In vivo evaluation

2.9.1. Animals

All animal experiments in this study were carried out in compliance with the Protocols of Animal Use and Care and were approved

by the Institutional Animal Ethics committee [Protocol No. ICT/IAEC/2012/P16 (Pharmacokinetic and brain uptake study); Protocol No. ICT/IAEC/2013/P66 (Toxicity Study)]. Rats were procured and acclimatized for seven days before commencement of the study. Animals were placed in polypropylene cages at controlled temperature 22 ± 1 °C and relative humidity of 60–70% and maintained with standard pellet diet (Amrut Brand, Sangli, India) and water ad libitum. Sprague-Dawley (SD) rats (male/female, ages 4–5 months) weighing between 200 and 250 g were selected for the study.

2.9.2. Drug administration

Rats were fasted for 12–16 h before the study with free access to water. The study was carried out in six groups of rats ($n = 4$), three groups for intranasal and three groups for intravenous administration. Prior to administration the rats were partially anesthetized by exposure to diethyl ether. DHA ME, Capmul ME and drug solution were administered intranasally and intravenously to rats. A drug solution of ABZ-SO and CUR was prepared dissolving ABZ-SO (1 mg/mL) and CUR (5 mg/mL) in a solvent system comprising propylene glycol:N,N-dimethylacetamide (95:5).

Rats were held by the neck with head tilted backwards during intranasal administration and formulations (50 μL) were instilled into the rat nostril with the help of a micropipette. For intravenous injection sample of 50 μL was diluted to 0.2 mL with PBS to facilitate ease of injection and was administered through the tail vein using a tuberculin syringe. The same dose ABZ-SO (0.2 mg/kg) and CUR (1 mg/kg) was administered by both routes.

2.9.3. HPLC method for bioanalysis

Reverse phase high performance liquid chromatography (RP HPLC) method to distinguish between CUR, its analogues and its degradation products to enable quantification of ABZ-SO and CUR was developed. The analysis of ABZ-SO and CUR was carried out using a HPLC system (Jasco PDA), which included 100 μL injection loop with C18 column Waters Spherisorb® 5 μm ODS2 (4.6 × 250 mm). Analytical column equipped with solvent delivery pump and Jasco MD-2010 multiwavelength detector was operated at 290 nm (ABZ-SO) and 425 nm (CUR). The mobile phase consisted of 2% glacial acetic acid (pH 3) and ACN in a ratio of 75:25 for ABZ-SO and 50:50 for CUR, pumped at a flow rate of 0.9 mL/min. The column was maintained at 25 °C and detection was carried out at 290 nm (ABZ-SO) and 425 nm (CUR).

Stock solution of ABZ-SO and CUR was prepared by dissolving accurately weighed drugs in methanol, to yield a concentration of 1 mg/mL. Working solutions of ABZ-SO and CUR were prepared by appropriate dilution with methanol. The method was validated for linearity, precision, accuracy, limit of detection (LOD) and limit of quantification (LOQ). The recovery of ABZ-SO and CUR was determined as follows: ABZ-SO and CUR were spiked to blank plasma or brain homogenate to give ABZ-SO and CUR concentrations of 20, 200, 500 and 1000 ng/mL. The analysis was performed using the method described above. Recovery was calculated by comparing the peak-area of the extracted sample to that of the unextracted standard solution containing the same concentration.

2.9.4. Drug extraction

Brain samples were homogenized using a tissue homogenizer in PBS:ACN (50:50) and centrifuged at 10,000*g* for 10 min to obtain the supernatants. Deproteination of plasma/brain supernatant was carried out in a 1.5 mL Eppendorf tube, 200 μL of plasma/brain homogenates supernatant and 300 μL of methanol were mixed and vortexed. 500 μL of 2% acetic acid (pH 3):ACN (75:25) was added to the deproteinated mixture and vortexed for 3 min. The precipitated proteins were separated by centrifugation at 20,000*g* for 10 min and supernatant was analysed for ABZ-SO and CUR by the validated HPLC method reported in Section 2.9.3.

2.9.5. Pharmacokinetic study

Blood (500 μL) was collected from the retro-orbital plexus into heparinized tubes at various time points of 0.083, 0.25, 0.5, 1, 2, 8, 24 h after dosing. Plasma was separated by centrifuging for 5 min at 5000*g*, and stored at −70 °C until HPLC analysis. The extraction of ABZ-SO and CUR was carried out as detailed in Section 2.9.4 and supernatant was analysed by the validated HPLC method as reported in Section 2.9.3.

2.9.6. Brain uptake study

For the brain uptake study, rats were euthanized at 0.25, 0.5, 1, 8, and 24 h by exposure to excess CO_2. Subsequently, the brains were isolated, washed twice using normal saline solution, made free from adhering to tissue/fluid and weighed. Samples were stored at −70 °C prior to HPLC analysis.

Drug extraction is detailed in Section 2.9.4. Supernatant was analysed by HPLC detailed in Section 2.9.3.

2.9.7. Targeting efficiency

Drug targeting efficiency [DTE] and direct transport percentage [DTP] indexes were adopted [34]. DTE was calculated using the following equation:

$$\%\mathrm{DTE} = (\mathrm{Bi.n./Pi.n.})/(\mathrm{Bi.v./Pi.v.}) \times 100 \quad (2)$$

where Bi.n. = AUC_{0-24} [brain] following intranasal administration, Pi.n. = AUC_{0-24} [Plasma] following intranasal administration, Bi.v. = AUC_{0-24} [brain] following intravenous administration, Pi.v. = AUC_{0-24} [Plasma] following intravenous administration.

In order to clarify nose to brain direct transport more clearly, direct transport percentage [DTP] is calculated using the following equation:

$$\mathrm{DTP}\ [\%] = \mathrm{Bi.n.} - \mathrm{Bx/Bi.n.} \times 100 \quad (3)$$

where Bx is the brain AUC fraction contributed by systemic circulation through the BBB following intranasal administration and

$$\mathrm{Bx} = [\mathrm{Bi.v./Pi.v.}] \times \mathrm{Pi.n.} \quad (4)$$

2.9.8. Subacute toxicity and nasal toxicity

Male SD rats ($n = 8$) were divided into seven groups of which groups I, II and III were administered formulations intravenously through tail vein while groups IV, V, VI, and VII received the formulation by intranasal administration as described in Section 2.9.3. Groups as indicated were as follows: group I: ABZ-SO CUR DHA ME (0.2 mg/kg ABZ-SO, 1 mg/kg of CUR), group II: Blank DHA ME, group III: vehicle control (Saline) for intravenous, group IV: ABZ-SO CUR DHA ME (0.2 mg/kg ABZ-SO, 1 mg/kg of CUR), group V: Blank DHA ME, group VI: vehicle control (Saline), and group VII positive control (1% Sodium deoxycholate w/v) for intranasal [35]. All groups were administered daily single intranasal dose (50 μL/nostril) or intravenous dose (50 μL was diluted to 0.2 mL with PBS) for 7 or 14 consecutive days. All animals were monitored for mortality, abnormal breathing and unusual behavior, till 14 days. Blood was collected from the retro orbital plexus on day 7 and day 14 for haematology and serum biochemistry. Four animals from each group were sacrificed at the end of day 7 and day 14 and organs such as brain, liver, lung, spleen, kidney and heart were isolated. Nasal tissues were excised from the groups administered the MEs, vehicle control and positive control intranasally. Tissues were decalcified paraffin embedded and sliced using a microtome [36]. Haematoxylin and eosin (H and E) stained sections of the nasal tissues and mucociliary were examined under an optical microscope (Nikon Fx-35A, Japan). All the organs were fixed in 10%v/v formalin solution, embedded in wax, microsectioned and stained with H and E and histopathological examination carried out.

2.10. In vitro efficacy evaluation on T. solium cyst.

2.10.1. Isolation and in vitro culture of cyst

Taenia solium (*T. solium*) cysts were obtained from naturally infected pigs slaughtered following approved protocols in Deonar abattoir, Mumbai, India. *T. solium* cysts were carefully isolated and cysts with fluid and intact bladder wall were collected. The isolated cysts were washed with PBS and transferred into individual wells of 12 well culture plates containing culture medium. Culture medium was prepared with RPMI 1640 medium supplemented with L-glutamine (2 mM), HEPES buffer (25 mM; Gibco), penicillin (10,000 U/mL), streptomycin (10 mg/mL), amphotericin B (0.25 mg/mL) and 10% foetal bovine serum.

2.10.2. Drug treatment

DHA MEs of ABZ-SO and CUR 1000 μg/mL were prepared separately and diluted with culture medium to obtain 5, 10, 100, 500, and 1000 ng/mL of ABZ-SO and CUR respectively. Drug free DHA ME and drug free Capmul ME were also evaluated. Control wells comprised cysts maintained in culture medium. The culture medium from all other wells was withdrawn and replaced with 2 mL of test formulations ABZ-SO DHA ME (5, 10, 100, 500, 1000 ng/mL), CUR DHA ME (5, 10, 100, 500, 1000 ng/mL), ABZ-SO: CUR (100:10 ng/mL) DHA ME, blank DHA ME and blank Capmul ME corresponding to 1000 ng/mL dilution ($n = 6$). Plates were incubated for 96 h at 37 °C in 5% CO_2.

2.10.3. Cyst size

Cyst size was monitored at 6, 24, 48, 72 and 96 h by measuring maximal length and maximal width of the cysts using a scale placed on the cover of the well plate and the average diameter was calculated. Photographs of the cysts were recorded at the above time intervals up to 72 h.

2.10.4. Alkaline phosphatase (ALP) estimation

Test samples from each well were withdrawn at 6, 24, 48, 72 and 96 h in 2 mL Eppendorf tube for ALP estimation and then wells were replenished with 2 mL of fresh test samples. The concentration of ALP in culture supernatants of *T. solium* cysts was determined using a commercially available colorimetric ALP detection system (Prietest Kit, Robonik, India), adapted to a microassay format. Readings were carried out by using rate of change of absorbance of sample against distilled water. Briefly, reagent 1 (800 μL) and reagent 2 (200 μL) were mixed and incubated at 37 °C for 2 min. Subsequently, 20 μL of supernatant from each well was added to this reagent mixture. After incubation at 37 °C for 60 s the rate of change of absorbance per minute (ΔA/min) for a period of 180 s was measured at 405 nm. Wells with culture medium containing only cysts served as control. The ALP level is expressed as unit/liter (U/L).

2.10.5. Histopathological evaluation by microscopy

Histopathological evaluation of the cysts for all test samples was carried out by microscopic analysis. *T. solium* cysts were withdrawn from culture medium, placed on glass slide, fixed with 10% formaldehyde, stained with H and E for all test samples and observed under a light microscope.

2.11. Statistical analysis

All data are expressed as mean ± SD. For multiple-group comparison, one-way ANOVA was used followed by Dunnett's test (GraphPad Prism 5, USA software). Specific comparison between groups was carried out using the unpaired Student's *t*-test (two tailed). All data were dose and weight normalized. Pharmacokinetic parameters for formulations were calculated using Basica software. Differences were considered statistically significant at $P < 0.05$.

3. Results and discussion

NCC cure rates are relatively low as well as slow with currently available regimens; further, the long term therapy necessitated, is complicated by side effects of the corticosteroids [9]. Intranasal administration is conceived as the strategy to bypass the formidable BBB and achieve high drug concentration in the brain, a prime requisite for improved therapy. Unlike standard oral administration of ABZ, we have resourcefully selected ABZ-SO the active metabolite as the drug, to circumvent the issue of limited metabolizing enzymes of ABZ in the nasal epithelium. CUR is conceived as a safer alternative to the corticosteroids. We therefore present a novel combination of ABZ-SO and CUR for NCC therapy.

Intranasally administered drugs enter the brain directly through the olfactory neuroepithelium by paracellular or transcellular pathways or by neuronal transport via the trigeminal pathway [1,19]. MEs could enhance such transport across the nasal mucosa more specifically if the globule size is low; further, ME components could also exert a positive effect on transport [15]. Our ME comprised a DHA rich oil wherein DHA could enhance both paracellular and transcellular permeability through the nasal mucosa. Furthermore the anti-inflammatory property of DHA [37] and its role as a brain nutrient provide added advantage in the therapy of NCC which affects the brain.

3.1. Solubility study

Maximum solubility of both ABZ-SO and CUR was seen in tween 80 (surfactant) and Capmul MCM (oil). Solubility in the DHA rich oil however was low for both drugs. A combination of Capmul MCM and the DHA rich oil revealed significant enhancement in solubility. Furthermore in case of ABZ-SO the solubility in Capmul MCM and the combination of DHA rich oil: Capmul MCM (1:1) was comparable (Fig. 1). While tween 80 and Capmul MCM were selected as the ME components based on the solubility of the drugs, DHA rich oil was selected due to the value added property of enabling targeted nose to brain delivery. Among the CoS maximum solubility was seen in polyethylene glycol (PEG) 400. Nevertheless all the three surfactants were evaluated, specifically as CoS is known to play a critical role in enhancing microemulsification.

3.2. Preparation and characterization of microemulsions

3.2.1. Phase behavior

Ethanol enabled larger ME region compared to PEG 400 and propylene glycol and hence was selected as CoS. Pseudoternary phase diagrams with tween 80:ethanol (S_{mix}) in the ratio of 3:1 and different oil phases are depicted in Fig. 2. The area of ME region increased with increasing ratio of tween 80:ethanol from 1:1 to 3:1. Significantly large ME region was obtained with Capmul MCM, a mixture of glycerol mono and dicaprate and medium chain triglycerides (Fig. 2A). DHA rich oil being a long chain triglyceride exhibited poor penetration into the surfactant monolayer and revealed a very small ME region as seen in the pseudoternary phase diagram (Fig. 2B). A combination of DHA rich oil and Capmul MCM (1:1) revealed significantly higher microemulsification and nearly doubled the ME region compared to only DHA rich oil (Fig. 2C), enabling development of ME comprising the DHA rich oil.

3.2.2. Drug loaded microemulsions

Drug loading up to 3 mg of ABZ-SO and 10 mg/mL of CUR (Fig. 3A) was feasible in the ME. Nevertheless ABZ-SO at a concentration greater than 2 mg/mL and CUR greater than 7 mg/mL revealed precipitation of the drugs following aqueous dilution as

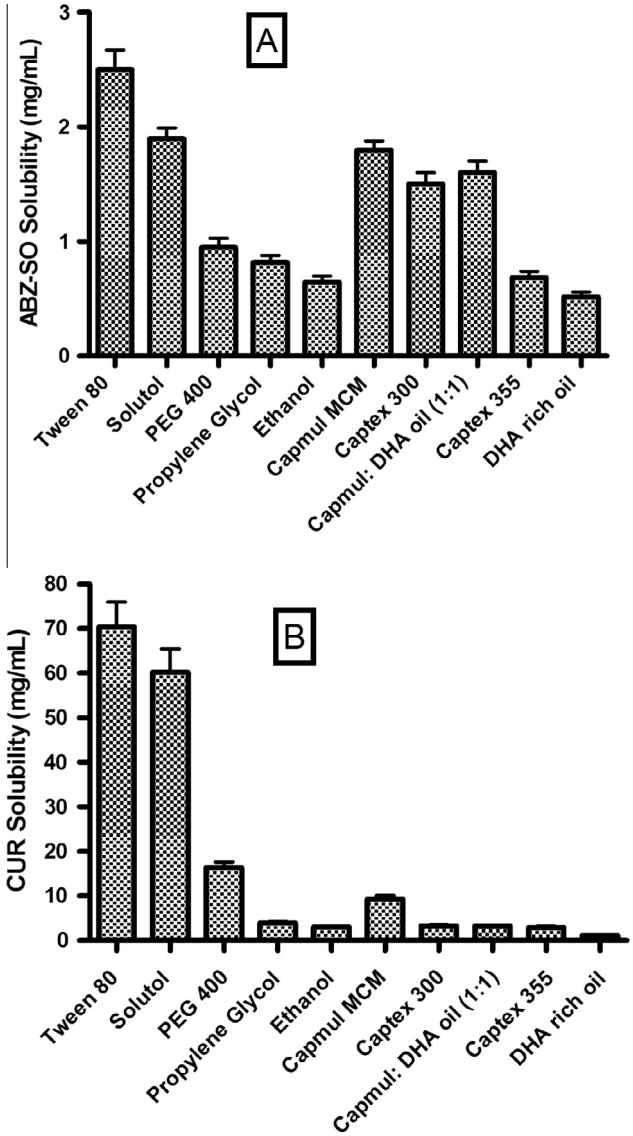

Fig. 1. Solubility of ABZ-SO (A) and CUR (B) in ME components.

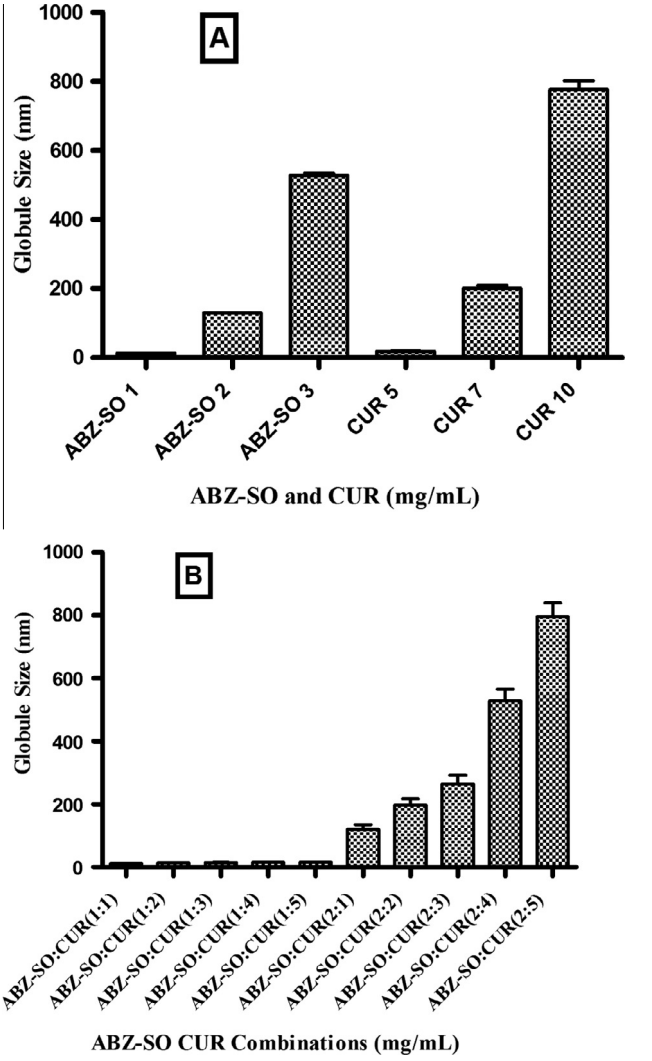

Fig. 3. Effect of drug loading on globule size of DHA ME (A) ABZ-SO and CUR, (B) ABZ-SO and CUR combinations.

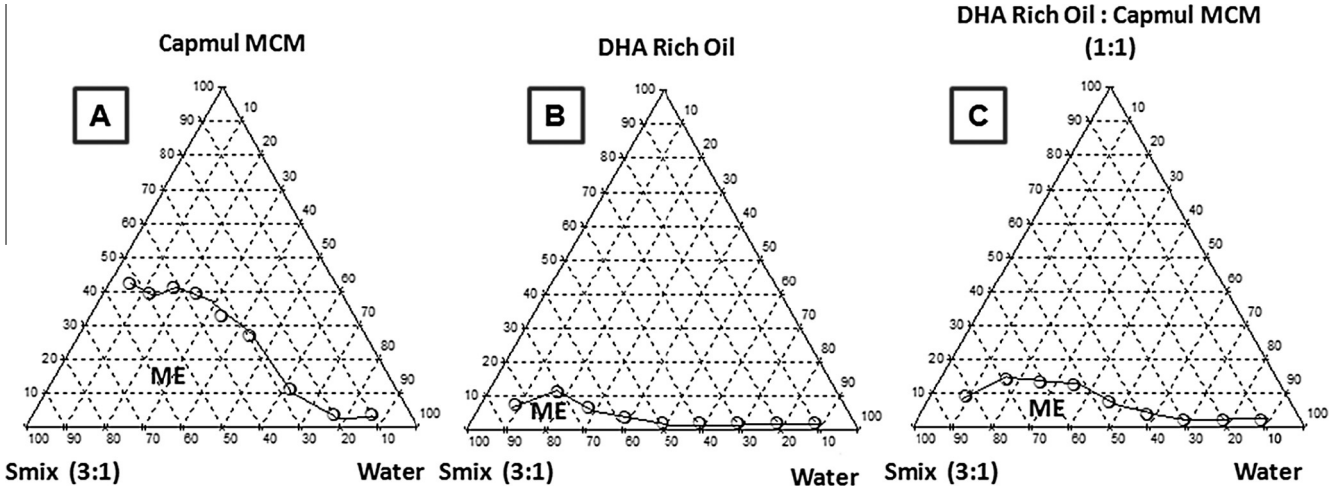

Fig. 2. Pseudoternary phase diagram of Tween 80:ethanol [S_{mix}] (3:1) (A) oil:Capmul MCM, (B) oil:DHA rich oil, (C) oil:DHA rich oil:Capmul MCM (1:1).

evident from the marked increase in size. Fig. 3B reveals the effect of drug concentration on the globule size of ME following 1:50 dilution with water. Maintaining ABZ-SO at 2 mg/mL it was not possible to incorporate CUR and similarly with CUR at 7 mg/mL incorporation of ABZ-SO was not feasible, as the combination of MEs revealed marked increase in size and also instantaneous precipitation on dilution in some cases. Hence the ME comprising a combination of ABZ-SO 1 mg/mL and CUR 5 mg/mL was arrived at.

3.2.3. Characterization

Physicochemical properties of the MEs are depicted in Table 1. The MEs were stable on dilution (50× and 100×) with average globule size <20 nm and negative zeta potential. The small globule size (<20 nm) and low polydispersity indices for MEs indicated that the ME approached a monodisperse stable system and could deliver the drug effectively owing to large surface area, while the negative zeta potential confirmed stability. The presence of zeta potential to the tune of −8.25 ± 0.77 and −10.4 ± 0.93 mV on the globules of Capmul ME and DHA ME, respectively, conferred physical stability to the system. Zeta potential is the main indicator of emulsion stability, and in zeta potential higher than −12 mV the emulsion tends to destabilize. As all the excipients used were non-ionic in nature, low zeta potential values could be attributed to the drug molecules [17–20]. The pH of all the ME formulations was well within the nasal pH range.

TEM (Fig. 4) micrograph of ME confirmed the spherical shape of the droplets (<20 nm). This was further confirmed by SANS analysis which showed polydisperse spheres with a radius of 36 Å (3.6 nm) and a polydispersity index of 0.2 (Fig. 5). SANS technique

Table 1
Physicochemical properties of microemulsions.

Formulation	Dilution	Capmul ME	DHA ME
Globule size (nm)	1:50	14.7 ± 1.12	16.4 ± 0.96
	1:100	15.64 ± 0.82	17.6 ± 1.02
Polydispersity index (PDI)	1:50	0.272 ± 0.05	0.258 ± 0.08
	1:100	0.267 ± 0.034	0.283 ± 0.023
Zeta potential (mV)	1:50	−8.25 ± 0.77	−10.4 ± 0.93
	1:100	−10.21 ± 0.88	−9.84 ± 0.68
Viscosity (cp)		170 ± 2.64	176 ± 2.11
pH		5.3 ± 0.44	5.6 ± 0.51
Mucoadhesion (g)		103.4 ± 3.13	110.47 ± 4.31
Drug content (%)	ABZ-SO	99.21 ± 2.3	99.97 ± 2.04
	CUR	99.67 ± 2.2	97.34 ± 2.4

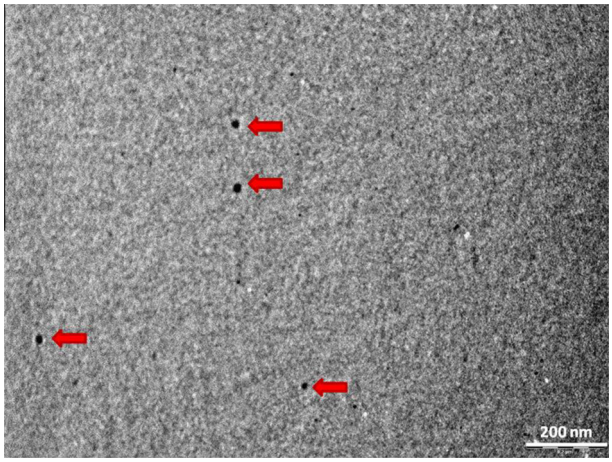

Fig. 4. TEM micrograph of ABZ-SO CUR DHA ME.

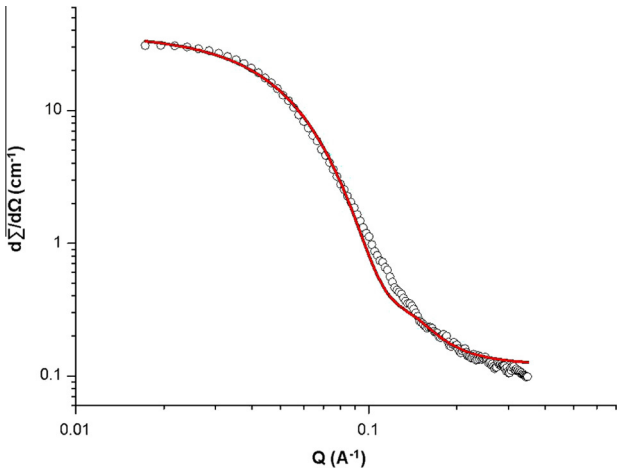

Fig. 5. SANS Image of ABZ-SO CUR DHA ME.

has been proved to be unique and powerful tool in elucidating the structure, interaction and phase transitions in lyophilic colloids especially in micellar and ME system. SANS analysis confirmed spherical droplets and no other surfactant mesophases. An important feature of an intranasal drug delivery system is its permanence in the nasal mucosa to evade the high mucociliary clearance, which has a speed of 5 mm/min in healthy humans [38,39]. The mucoadhesive property of MEs (Table 1), although surprising provides the important advantage of nasal mucoretention to deliver sustained drug concentration to the brain. The viscosity of MEs was suggested suitable for intranasal administration.

3.2.3.1. Fourier Transform Infrared (FTIR) Spectroscopy. Fig. 6 represents FTIR Spectrum of ABZ-SO (A), CUR (B) and ABZ-SO CUR DHA ME (C). FTIR of ABZ-SO drug powder revealed all the characteristic frequencies and vibrational assignments of ABZ-SO. Secondary amine absorption band seen at 3020 cm^{-1}, C═O at 1726 cm^{-1}, S═O at 1215 cm^{-1} for ABZ-SO (Fig. 6A). The infrared spectrum of CUR drug powder exhibited an O—H stretching at 3437 cm^{-1}, C—H stretching absorption bands at 2856 and 2924 cm^{-1}, an enol carbonyl stretching absorption band at 1622 cm^{-1}, —C—H bending absorption band at 1456 cm^{-1} and C—O stretching absorption band at 1126 cm^{-1} (Fig. 6B). FTIR of ABZ-SO and CUR drug powder revealed all the characteristic frequencies and vibrational assignments of ABZ-SO and CUR respectively. The infrared spectrum of the ABZ-SO CUR DHA ME exhibited an O—H stretching at 3394.72 cm^{-1}, C—H stretching absorption bands at 2866 and 2924 cm^{-1}, an enol carbonyl stretching absorption band at 1732 cm^{-1}, —C—H bending absorption band at 1463 cm^{-1} and C—O stretching absorption band at 1103 cm^{-1}. These peaks are in accordance with the structure and functional groups of ABZ-SO and CUR confirming the chemical stability of the drug and no chemical interaction between drug and excipient in the ME (Fig. 6C).

3.3. Stability evaluation

ABZ-SO CUR MEs subjected to freeze–thaw cycling exhibited no change in color, no precipitation or change in globule size on dilution. Drug content >95% for both drugs was evident at the end of 6 months even after exposure to 40 °C/75% RH as per ICH guidelines, confirming good stability.

3.4. Haemolysis and serum stability

MEs exhibited low per cent haemolysis (<10%) [40] and no significant increase in globule size ($P > 0.05$) over a period of 6 h

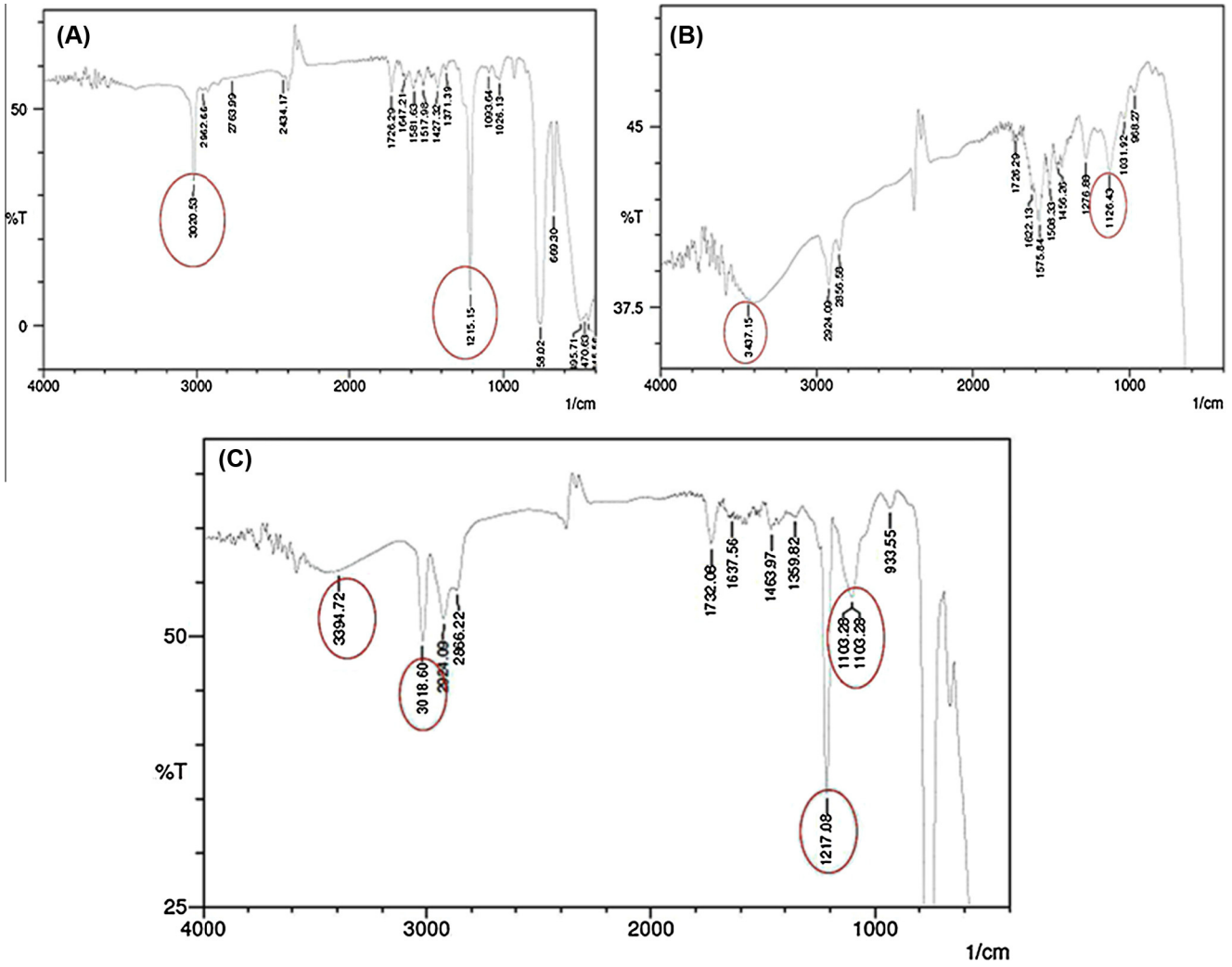

Fig. 6. FTIR Spectrum of ABZ-SO (A), CUR (B) and ABZ-SO CUR DHA ME (C).

in serum indicating good stability and safety for intravenous administration.

3.5. Ex vivo permeation studies through sheep nasal mucosa

The ME formulations favoured an increase in drug permeability coefficient and steady state flux (f_{ss}) compared to drug solution (Fig. 7). Further significant and rapid permeation of both the drugs ($P < 0.05$) was seen with the DHA ME compared to the Capmul ME and drug solution, as evident from the f_{ss}, flux enhancement ratio and permeability coefficient (P) (Table 2).

The high ex vivo permeation of DHA ME across the nasal mucosa could be attributed to both paracellular and transcellular transport. Improved paracellular diffusion is reported by Hossain et al. in their study with highly unsaturated omega 3-enriched phosphatidylcholine liposomes [41]. The disruption of epithelial barrier function by DHA to enhance the tight junction permeability and increase paracellular permeation is partly mediated by the phospholipase C (PLC)/Ca^{2+}/protein kinase C (PKC) pathway and by the formation of eicosanoid [42,43]. Further, increase in DHA mediated lipid peroxidation with the formation of hydrogen peroxide and peroxynitrite, could also disrupt the epithelial barrier function [43]. The ability of DHA to alter membrane fluidity could enable transcellular transport. Further hydrolysis of the triglycerides to DHA (free fatty acid) may have been possible in the tissue. These factors could have positively contributed to DHA mediated enhancement in tight junction permeability. Nevertheless the significant enhancement seen with DHA ME suggested that DHA played an important role in enhancing permeation across the nasal mucosa. Tween 80 which also influences the tight junction permeability could have additionally contributed to increased nasal permeation of the drugs [44].

3.6. In vivo evaluation

3.6.1. HPLC method for bioanalysis

A mobile phase comprising of 2% glacial acetic acid (pH 3):ACN (75:25) enabled good resolutions and peak symmetry of ABZ-SO while a composition of 50:50 enabled good resolution of the three curcuminoids. All the analytes were well separated with a peak symmetry factor <1 and retention time of 8 ± 0.27 min for ABZ-SO, and 11.55 ± 0.28, 12.95 ± 0.36 and 13.28 ± 0.25 min respectively for bisdemethoxycurcumin, demethoxycurcumin and curcumin. The calibration curves were linear in the concentration range of 25–2000 ng/mL for both drugs. Limit of detection (LOD) and limit of quantification (LOQ) for rat plasma and brain homogenate were 5 and 10 ng/mL respectively for ABZ-SO and CUR. The ability of the method to separate ABZ-SO and CUR from plasma/brain homogenate products indicated specificity of the method. The method showed a RSD of <3 suggesting precision.

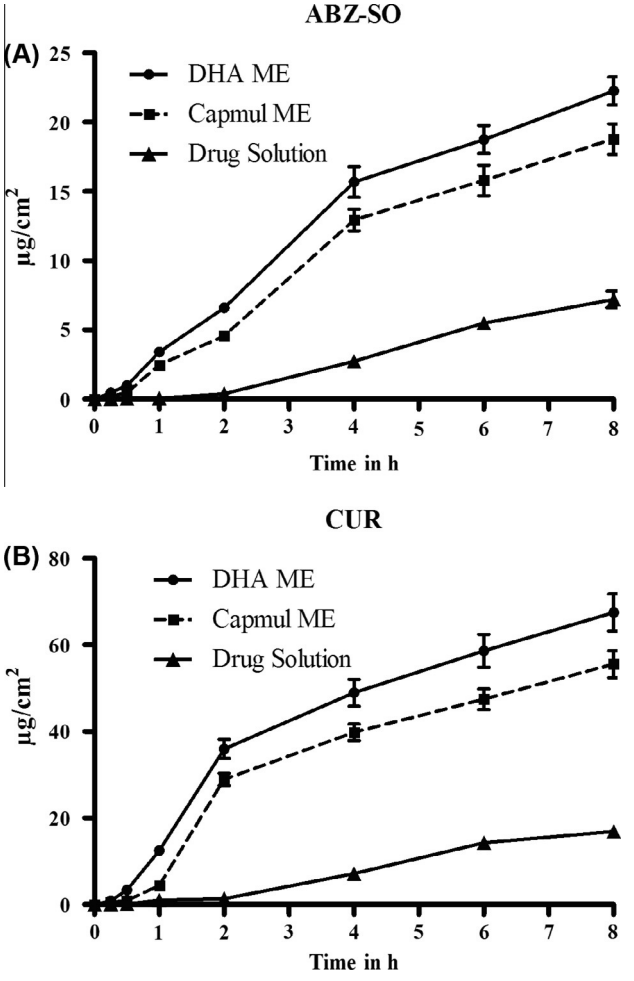

Fig. 7. Ex vivo permeation vs. time profile across nasal mucosa of ABZ-SO (A) and CUR (B) from MEs or drug solution.

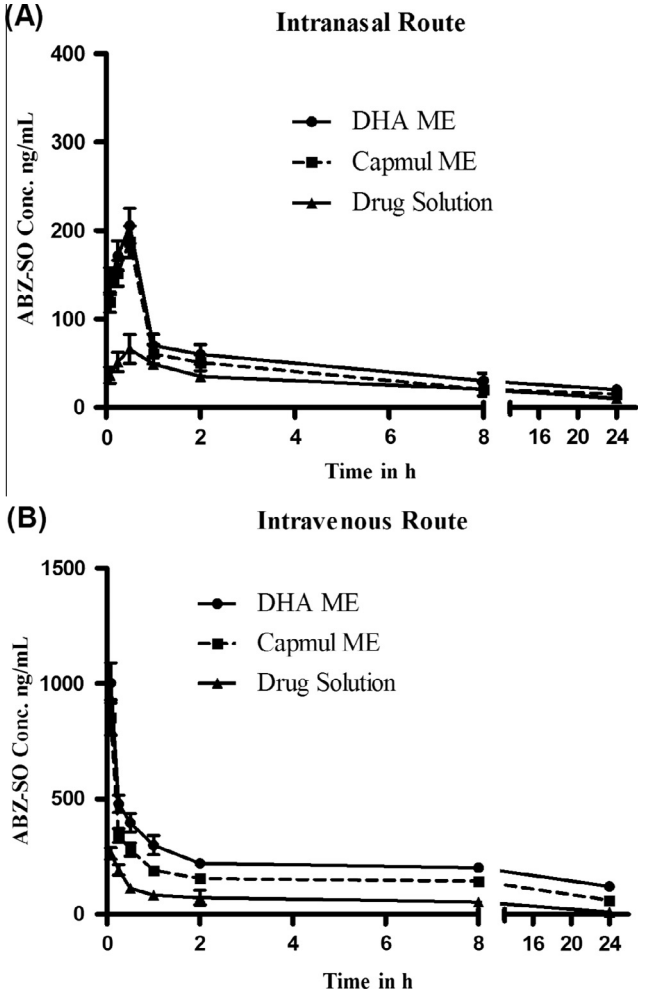

Fig. 8. Plasma ABZ-SO concentration vs. time profiles following intranasal (A) and intravenous (B) administration of the drug in MEs or drug solution to SD rats.

Table 2
Ex-vivo drug permeation across sheep nasal mucosa.

	ABZ-SO			CUR		
	Drug solution	Capmul ME	DHA ME	Drug solution	Capmul ME	DHA ME
Steady state flux (f_{ss}), (µg cm^{-2} h^{-1})	0.8444 ± 0.17	2.5428 ± 0.34	3.0533 ± 0.41	2.0903 ± 0.17	7.8263 ± 0.34	9.6751 ± 0.41
Enhancement ratio	–	3.01 ± 0.21	3.6159 ± 0.28	–	3.744 ± 0.21	4.6285 ± 0.28
Permeability coefficient (cm/h)	0.0168	0.05085	0.06106	0.008361	0.0313	0.0387

3.6.2. Drug extraction

Extraction of ABZ-SO and CUR from plasma and brain homogenate was consistent and reproducible. Extraction efficiency was optimized and recovery of extracted sample from plasma and brain homogenate was found to be greater than 90%, when analyzed by the reported HPLC method.

3.6.3. Plasma pharmacokinetics

Plasma pharmacokinetics ABZ-SO and CUR following intravenous and intranasal administration are depicted in Figs. 8 and 9 respectively. Intranasal delivery revealed rapid absorption with an early t_{max} (time to reach C_{max}) for both ABZ-SO and CUR from the MEs; nevertheless, plasma drug levels were very low compared to intravenous ($P < 0.05$). Following intranasal administration maximum concentration (C_{max}) was lower than the plasma concentration achieved with intravenous administration at 24 h, suggesting the possibility of high targeting to the brain. On the other hand high plasma level was seen following intravenous administration of the DHA ME, exhibiting significantly lower elimination and longer circulation ($t_{1/2}$) for both drugs compared to Capmul ME (Tables 3 and 4). DHA being a long chain triglyceride provides longer circulation due to slow metabolism [45–47].

3.6.4. Brain pharmacokinetics

Rapid brain uptake with significantly higher drug concentrations of ABZ-SO (Fig. 10A) and CUR (Fig. 11A) was observed following intranasal administration of the MEs ($P < 0.05$). Nevertheless the C_{max} obtained with the DHA ME was significantly higher. Furthermore significantly longer $t_{1/2}$ and lower elimination rate also suggested sustained drug concentrations with the DHA ME [47]. Similar behavior was seen with the Capmul ME; nevertheless, C_{max} was significantly lower than that of the DHA ME indicating lower uptake faster drug elimination from the brain ($P < 0.05$) (Tables 5 and 6). In contrast intravenous formulations revealed slower and lower brain uptake [Fig. 10B (ABZ-SO) and Fig. 11B

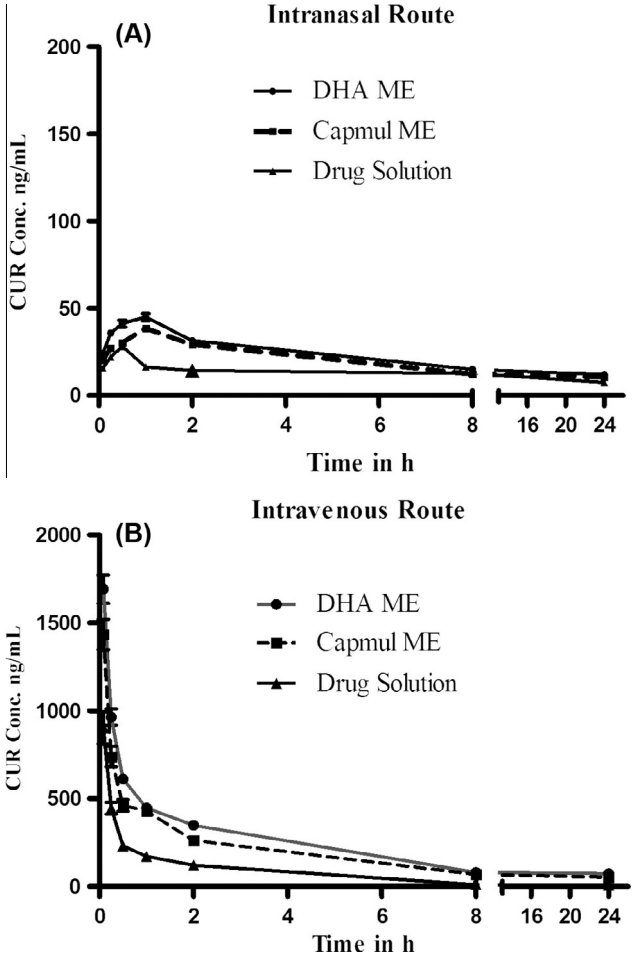

Fig. 9. Plasma CUR concentration vs. time profiles following intranasal (A) and intravenous (B) administration of the drugs in MEs or drug solution to SD rats.

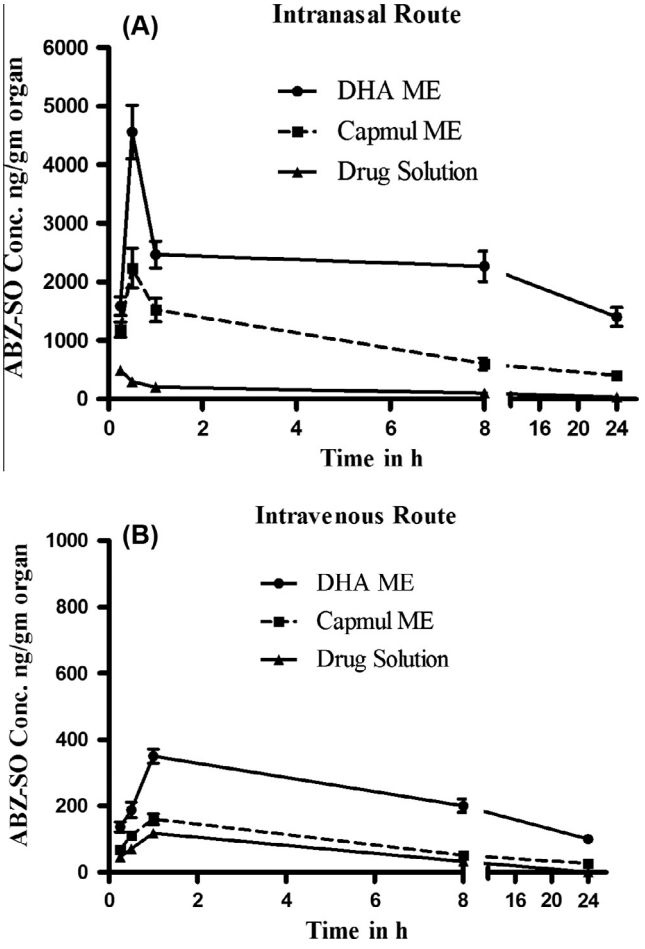

Fig. 10. Brain ABZ-SO concentration vs. time profiles following intranasal (A) and intravenous (B) administration of the drug in MEs or drug solution to SD rats.

(CUR)]. Intranasal DHA ME revealed a 20.4 fold enhancement in ABZ-SO concentration compared to the drug solution while significantly lower enhancement of 7.1 fold was seen with Capmul ME. Similarly enhancement of 5.1 fold and 2.67 fold was seen with DHA ME and Capmul ME respectively for CUR compared to drug solution.

The enhanced permeation seen in the ex vivo permeation was correlated in the in vivo study. In particular the high concentration seen with the DHA ME confirmed the important role of DHA in altering the barrier property of nasal epithelium to facilitate high drug targeting to the brain as confirmed by the high values of DTP which represents direct nose to brain transport. DTP for the

Table 3
Plasma pharmacokinetic parameters upon intravenous and intranasal administration of the MEs of ABZ-SO or drug solution in SD rats.

Parameters	Intravenous			Intranasal		
ABZ-SO	Drug solution	Capmul ME	DHA ME	Drug solution	Capmul ME	DHA ME
C_{max} (ng/mL)	263.34 ± 15.8	853.58 ± 21.63	1003.29 ± 53.58	66.19 ± 8.5	187.43 ± 12.73	205 ± 13.89
t_{max} (h)	0.0833	0.0833	0.0833	0.5	0.5	0.5
kel (h^{-1})	0.0991 ± 0.0051	0.0450 ± 0.0018	0.0284 ± 0.001	0.0544 ± 0.002.1	0.0781 ± 0.0029	0.0491 ± 0.0016
$t_{1/2}$ (h)	6.98 ± 0.42	15.38 ± 0.87	24.399 ± 1.05	10.78 ± 0.73	14.48 ± 0.91	15.44 ± 0.83
AUC_{0-24}	1083.60 ± 76.2	3000.4 ± 168.4	4553.16 ± 172.8	503.94 ± 20.5	682.31 ± 31.2	882.99 ± 42.3

Table 4
Plasma pharmacokinetic parameters upon intravenous and intranasal administration of the MEs of CUR or drug solution in SD rats.

Parameters	Intravenous			Intranasal		
CUR	Drug solution	Capmul ME	DHA ME	Drug solution	Capmul ME	DHA ME
C_{max} (ng/mL)	904.29 ± 36.3	1434 ± 62.1	1692 ± 69.6	28.31 ± 1.6	38.5 ± 2.2	45.04 ± 2.6
t_{max} (h)	0.0833	0.0833	0.0833	0.5	1	1
kel (h^{-1})	0.1071 ± 0.0084	0.0657 ± 0.0029	0.0574 ± 0.0022	0.0548 ± 0.0028	0.0389 ± 0.0018	0.0378 ± 0.0015
$t_{1/2}$ (h)	6.468 ± 0.34	10.166 ± 0.65	12.064 ± 0.81	12.2 ± 0.72	17.1 ± 0.65	18.355 ± 0.73
AUC_{0-24}	1040.29 ± 42.3	2932.3 ± 148.5	3682.84 ± 163.1	250 ± 10.7	370.017 ± 14.6	431.2356 ± 17.3

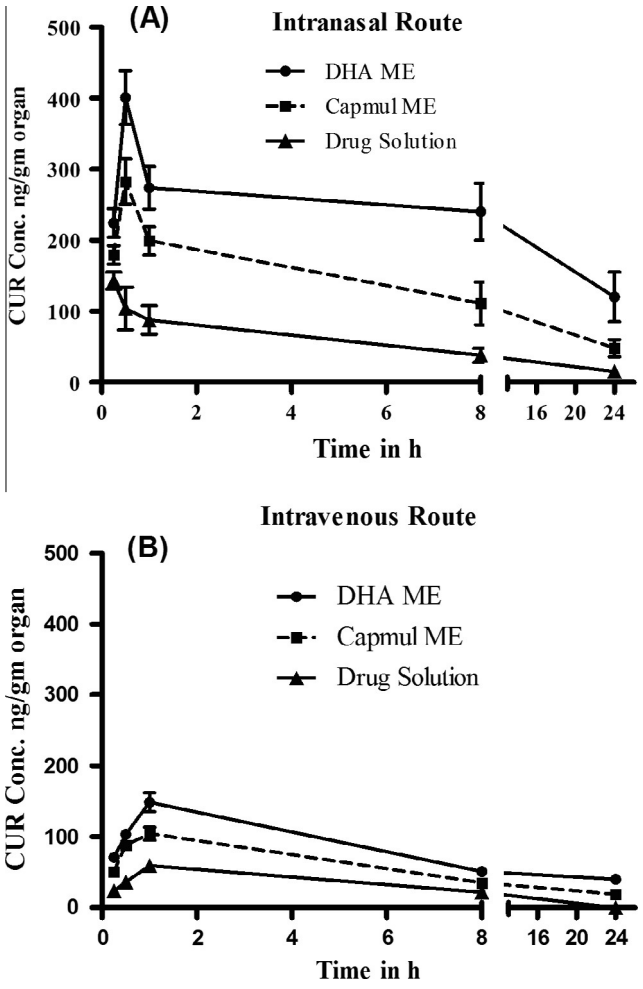

Fig. 11. Brain CUR concentration vs. time profiles following intranasal (A) and intravenous (B) administration of the drug in MEs or drug solution to SD rats.

MEs was very high and >95% and lower for the drug solution (Table 7). DTE represents a time-average partitioning ratio. The targeting efficiency for both drugs was significantly higher for MEs compared to the drug solutions with significantly higher DTE with DHA ME compared to Capmul ME. An enhancement of 2.9 fold for CUR and even greater enhancement of 11.6 fold for ABZ-SO were observed with DHA. The higher DTE and DTP suggest that DHA ME has better brain targeting efficiency mainly because of substantial direct nose-to-brain transport.

To understand whether the intranasal route provided advantage in enhanced brain concentration, we compared the brain uptake following intravenous administration of the same formulations. Our ME is comprised of DHA and tween 80, and it was therefore expected that intravenous formulation would also provide enhanced brain uptake because DHA being a nutrient and major component of the brain lipid has the natural endogenous transporter, major facilitator superfamily domain-containing protein 2a (Mfsd2a) to traverse the BBB [48]. Tween 80 is also reported to enable lipoprotein receptor mediated endocytosis across the BBB [49–51]. Following intravenous administration brain uptake of ABZ-SO and CUR was significantly lower compared to the corresponding intranasally administered formulations. For instance while intranasal DHA ME revealed brain C_{max} of a 4560 ± 460.3 ng/g (ABZ-SO), brain C_{max} following intravenous administration was <1/10th and barely 350.42 ± 21.2 ng/g. Difference in C_{max} for CUR was also high and significant; 400.98 ± 38.4 ng/g (intranasal) and 148.4 ± 13.3 ng/g (intravenous) ($P < 0.05$). Moreover following intranasal administration even at 24 h the DHA ME revealed a ABZ-SO concentration that was 4 fold (1400.2 ± 160.1 ng/g) the C_{max} following intravenous administration, while these values although not so high were comparable for CUR.

The high DTE values confirmed maximum targeting with the DHA ME followed by significantly lower targeting with Capmul ME compared to the drug solution (Table 7). While the enhancement ratio was very high for ABZ-SO it was lower for CUR. Furthermore the MEs play a crucial role in providing sustained brain concentration due to the mucoadhesive property. Mucoadhesive MEs could exhibit prolonged retention in the nasal mucosa thereby

Table 5
Brain pharmacokinetic parameters upon intravenous and intranasal administration of the ME of ABZ-SO or drug solution in SD rats.

Parameters	Intravenous			Intranasal		
ABZ-SO	Drug solution	Capmul ME	DHA ME	Drug solution	Capmul ME	DHA ME
C_{max} (ng/g)	118.02 ± 7.6	160 ± 5.8	350 ± 13.3	490.113 ± 23.8	2239.81 ± 87.5	4560 ± 165.3
t_{max} (h)	1	1	1	0.25	0.5	0.5
kel (h^{-1})	0.138 ± 0.0073	0.0902 ± 0.0068	0.0525 ± 0.0027	0.082 ± 0.0033	0.0525 ± 0.003	0.0225 ± 0.0013
$t_{1/2}$ (h)	5.00 ± 0.21	9.02 ± 0.36	13.18 ± 0.83	8.4 ± 0.52	13.2 ± 0.86	27.061 ± 1.2
AUC_{0-24}	595 ± 28.7	1456 ± 43.7	4517.18 ± 187.9	2382.765 ± 102.3	16953. 93 ± 683.2	48620.78 ± 1631.7
Relative bioavailability (%)[a]	–	244.7	759.189	400.46	2849.4	8171.559

[a] Intravenous drug solution as reference.

Table 6
Brain pharmacokinetic parameters upon intravenous and intranasal administration of the MEs of CUR or drug solution in SD rats.

Parameters	Intravenous			Intranasal		
CUR	Drug solution	Capmul ME	DHA ME	Drug solution	Capmul ME	DHA ME
C_{max} (ng/g)	59.37 ± 6.2	104.43 ± 8.6	148.4 ± 10.6	143.01 ± 11.4	282.856 ± 19.3	400.982 ± 27.8
t_{max} (h)	1	1	1	0.25	0.5	0.5
kel (h^{-1})	0.0997 ± 0.0065	0.0697 ± 0.0043	0.0498 ± 0.0035	0.0735 ± 0.0051	0.0597 ± 0.0032	0.0371 ± 0.0017
$t_{1/2}$ (h)	6.5 ± 0.42	10.1 ± 0.66	14 ± 0.82	9.420 ± 0.46	11.607 ± 0.75	18.654 ± 0.93
AUC_{0-24}	318.9 ± 20.1	994.93 ± 46.4	1520.7 ± 82.3	961.4184 ± 38.76	2567.25 ± 120.6	4953.11 ± 194.8
Relative bioavailability (%)[a]	–	311.98	476.85	301.47	805.032	1553.18

[a] Intravenous drug solution as reference.

Table 7
DTE (%) and DTP (%) after intranasal administration of ABZ-SO CUR MEs and ABZ-SO CUR drug solution.

	ABZ-SO			CUR		
	Drug solution	Capmul ME	DHA ME	Drug solution	Capmul ME	DHA ME
Drug targeting efficiency (DTE%)	860	4525.86	10029.81	1256.53	2267.38	3751.63
% Enhancement	–	5.262	11.662	–	1.804	2.985
Direct nose-to-brain transport (DTP%)	88.38	98.04	98.2	92.04	95.11	96.40

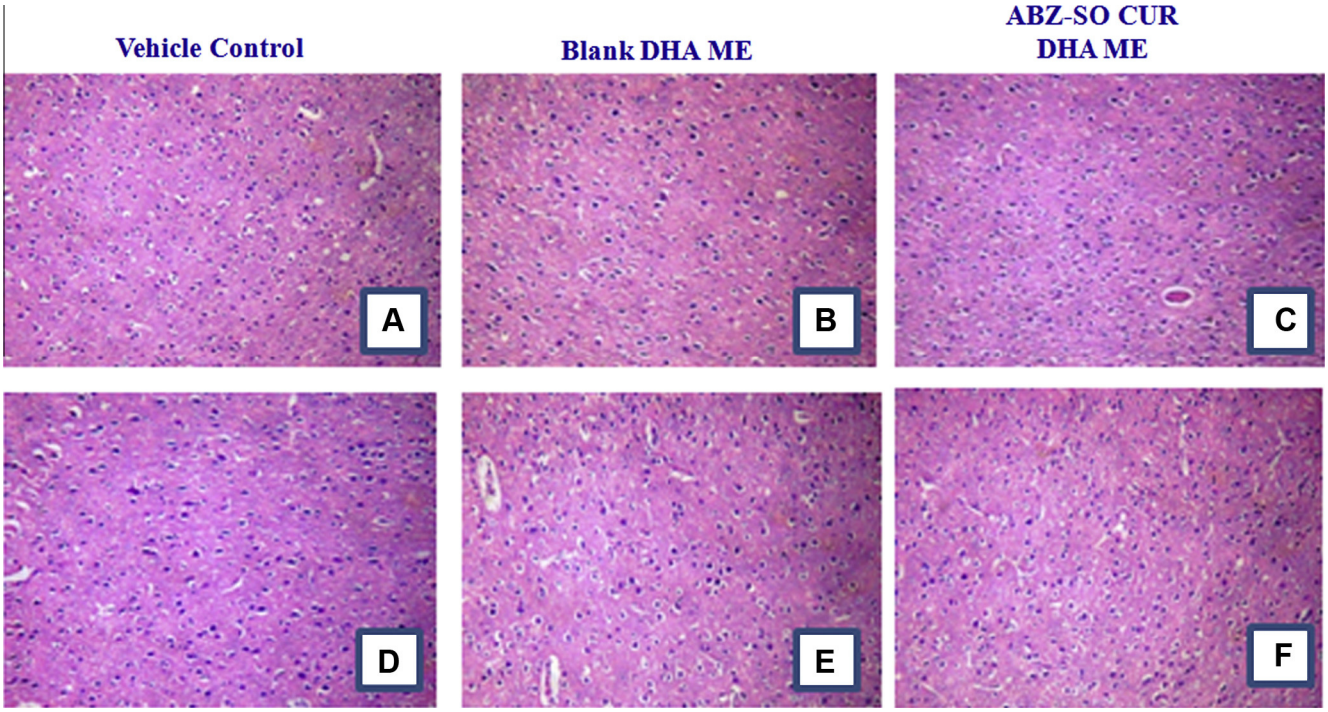

Fig. 12. Photomicrographs of brain following intravenous administration vehicle control (A, 14 days), blank DHA ME (B, 14 days)] and ABZ-SO CUR DHA ME (C, 14 days) and photomicrograph of brain following intranasal administration vehicle control (D, 14 days), blank DHA ME (E, 14 days) and ABZ-SO CUR DHA ME (F, 14 days) (10 × 10 magnification, $n = 4$).

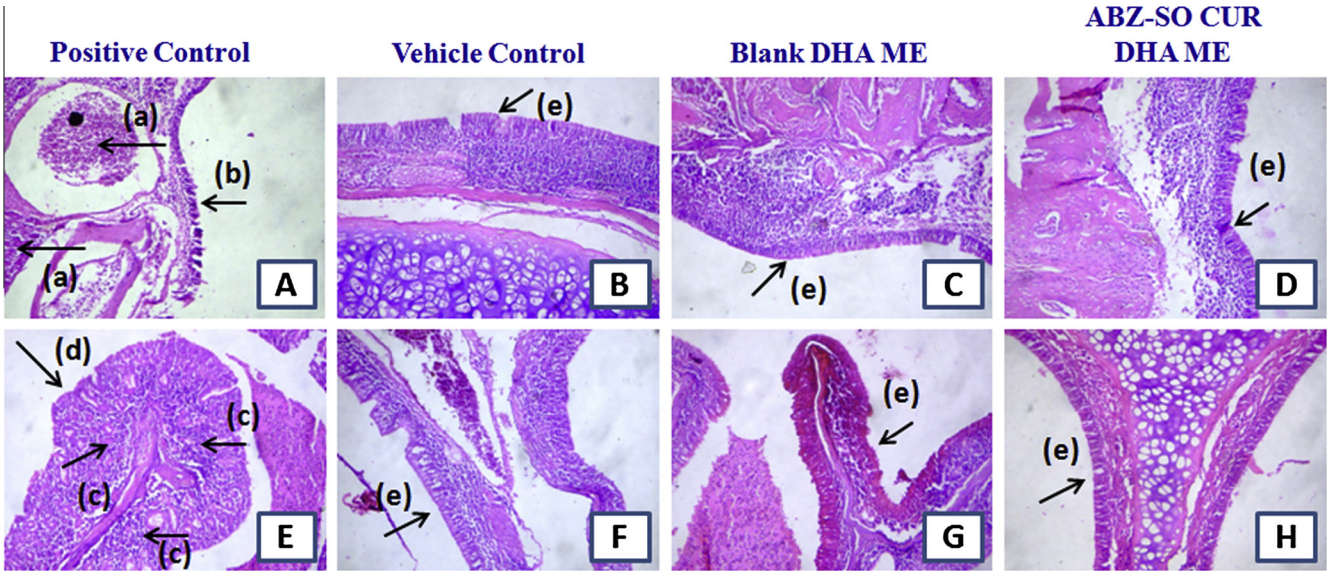

Fig. 13. Photomicrographs of positive control [1% sodium deoxycholate solution, (A, 7 days) (E, 14 days)], vehicle control [saline, (B, 7 days) (F, 14 days)], blank DHA ME [(C, 7 days) (G, 14 days)] and ABZ-SO CUR DHA ME [(D, 7 days) (H, 14 days)] (10 × 10 magnification). *(a) Moderate infiltration, (b) degenerative changes in nasal epithelium, (c) severe leucocytic infiltration, (d) extensive desquamation of nasal epithelium and (e) intact nasal epithelium with healthy appearance.

providing significant advantage in enabling sustained brain concentrations [5,16,17,20].

3.6.5. Subacute toxicity and nasal toxicity

Serum biochemistry and haematology data were comparable with the vehicle control at the end of 14 days. Histopathology of all vital organs including brain revealed healthy appearance and no significant changes at the end of 14 days. Fig. 12 depicts photomicrographs of the brain at the end of the study.

The nasal toxicity study also reflected no changes in nasal histopathology with vehicle control, blank DHA ME and ABZ-SO CUR DHA ME (Fig. 13). Nasal epithelium was intact and showed healthy appearance in subjects belonging to vehicle control and the test groups. The subjects from positive control group i.e. sodium deoxycholate, showed moderate to severe degree of leucocytic infiltration, degenerative changes in the nasal epithelium and desquamation of varying degree by day 7 (Fig. 13A). Similar changes were noted in the nasal passage of subjects belonging to positive control group in which treatment was extended to 14 days (Fig. 13E).

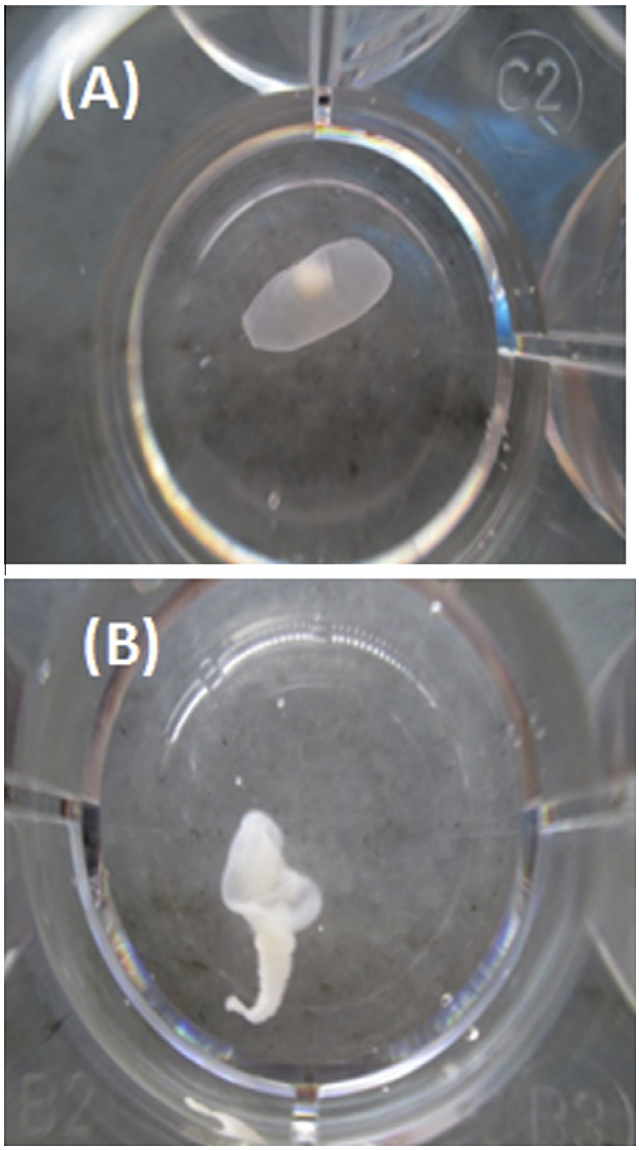

Fig. 14. Photograph of *T. solium* cyst (A) invaginated state and (B) evaginated state.

3.7. In vitro efficacy evaluation on T. solium cyst.

3.7.1. Changes in cyst size and alkaline phosphatase inhibition

Size and viability of cysts are critical parameters which indicate efficacy of treatment. Cysts remain initially in the invaginated state (Fig. 14A) and have an average diameter in the range 7–11 mm. Over a period of time viable cysts evaginate (Fig. 14B) and finally grow into a tape worm.

While evagination of cysts was evident at 5 ng/mL with ABZ-SO DHA ME and CUR DHA ME, at concentrations of 10 ng/mL and greater, no evagination was seen. Nevertheless a concentration and time dependent decrease in cyst size were observed only at concentrations of 100 ng/mL and greater. At equivalent concentrations the decrease in cyst size exhibited by ABZ-SO DHA ME was significantly greater than CUR DHA ME ($P < 0.05$). While blank Capmul ME showed marginal decrease in cyst size, a significant decrease in cyst was observed with blank DHA ME ($P < 0.05$) which was comparable with CUR DHA ME 100 ng/mL ($P > 0.05$). Further decrease in cyst size was comparable for ABZ-SO DHA ME 1000 ng/mL and ABZ-SO: CUR (100:10 ng/mL) DHA ME and complete disintegration of cysts was observed with ABZ-SO DHA ME at 500 and 1000 ng/mL and ABZ-SO: CUR (100:10 ng/mL) DHA ME at 96 h confirming efficacy of the formulations. ABZ-SO is a known cysticidal drug and hence cysticidal activity was anticipated. The decrease in cyst size seen with blank DHA ME suggested the cysticidal property of DHA. More specifically the high efficacy seen with ABZ-SO: CUR (100:10 ng/mL) DHA ME which was comparable with ABZ-SO DHA ME (1000 ng/mL), which had a 10 fold higher concentration of ABZ-SO suggests a high possibility that both DHA and CUR exerts some role in assisting cysticidal activity (Fig. 15).

Alkaline phosphatase (ALP) is an enzyme found in the cells and extracellular fluids of a wide range of organisms including helminth parasites. It is associated with absorption and/or digestion of food materials. Any interference in the level of this enzyme could result in paralysis or death of the parasites [11]. In view of its functional significance ALP inhibition is used as detection tool to determine damage to parasites or cysts [52].

In the drug free control wells ALP in the supernatant increased progressively up to 96 h confirming viability of the cysts. ABZ-SO DHA ME exhibited time and concentration dependent inhibition of ALP. Moreover at 96 h ALP was not detected from 500 and 1000 ng/mL of ABZ-SO DHA ME and ABZ-SO: CUR (100:10 ng/mL) DHA ME indicating mortality of cysts. Although ALP inhibition with CUR DHA ME (100 ng/mL) was lower it was comparable to blank DHA ME (Fig. 16). The results of ALP inhibition therefore correlated well with decrease in cyst size with high correlation coefficient (r^2) namely ABZ-SO DHA ME 1000 ng/mL (0.997), 500 ng/mL (0.944), 100 ng/mL (0.923), ABZ-SO and CUR (100:10 ng/mL) DHA ME (0.893) and CUR DHA ME 100 ng/mL (0.905).

Although the mechanism whereby DHA inhibits ALP activity is not clear short- and long-term DHA exposure to osteoblasts cells inhibited ALP activity [53] while omega-3 fatty acids inhibited ALP activity and mineralization of vascular cells [53]. This explains the activity seen with the blank DHA ME. The decrease in cyst size coupled with inhibition of ALP seen with the ABZSO: CUR DHA ME at a 10 fold lower ABZ-SO concentration is indeed surprising and also suggests the possibility that CUR contributes to cysticidal effect. Further the high efficacy of the combination of ABZ-SO: CUR (100:10 ng/mL) DHA ME also suggests a possible synergy between ABZ-SO and CUR.

The ratio of ABZ-SO: CUR (100:10) was selected based on the in vivo brain concentrations seen at 24 h following nasal administration of DHA ME namely 1400.2 ± 160.1 ng/g for ABZ-SO and 120 ± 35.2 ng/g for CUR. The high efficacy in vitro with the ABZSO

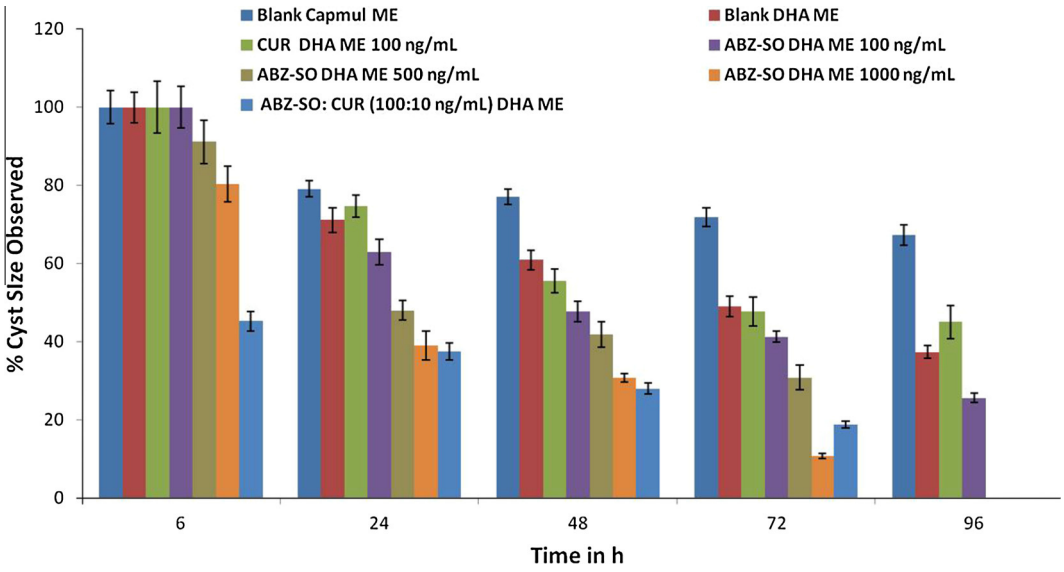

Fig. 15. Changes in the *T. solium* cysts size during treatment with blank Capmul ME, blank DHA ME, CUR DHA ME (100 ng/mL), ABZ-SO DHA ME (100, 500, 1000 ng/mL), ABZ-SO and CUR (100:10 ng/mL) DHA ME.

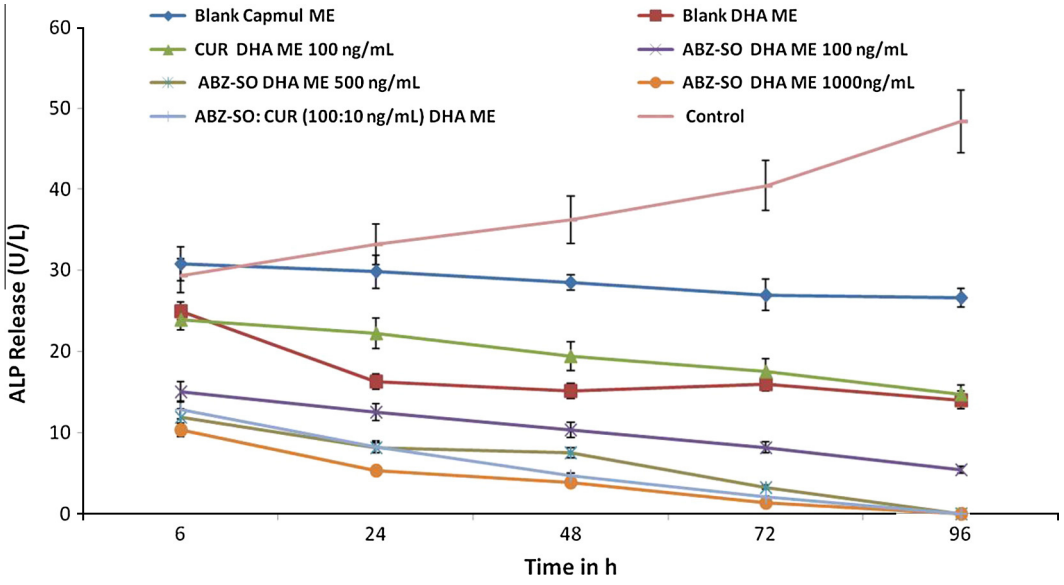

Fig. 16. Effects of treatment with blank Capmul ME, blank DHA ME, CUR DHA ME (100 ng/mL), ABZ-SO DHA ME (100, 500, 1000 ng/mL), ABZ-SO: CUR (100:10 ng/mL) DHA ME and control on in vitro release/secretion of ALP by *T. solium* cysts.

and CUR combination, at 10 fold lower drug concentrations achieved in the brain, reflected by complete ALP inhibition and disintegration of cysts at 96 h, strongly supports the validity of the assumption of clinical efficacy at the concentrations achieved in vivo.

3.8. Histopathological evaluation by microscopy

The morphological alterations of the *T. solium* cysts were monitored by light microscopy. Control cysts remained unaltered showing classical movements and normal appearance. Following drug treatment the cyst showed clear morphological alterations in the tissue in contrast to the control group. Control group revealed unchanged cyst wall (Fig. 17A1), normal cyst wall with compact parenchyma (Fig. 17B1), intact tegumental wall (Fig. 17C1) and presence of microtriches (Fig. 17D1). Treatment groups revealed cyst wall degeneration and breakage in the cyst wall at many locations (Fig. 17A2-ABZ-SO DHA ME, A3-blank DHA ME), vacuolization in cyst parenchyma (Fig. 17B2-ABZ-SO DHA ME, B3-blank DHA ME), and destruction and disintegration of the tegumental wall (Fig. 17C2-ABZ-SO DHA ME, C3-blank DHA ME). The microtriches disappeared in some zones and the germinal layer was visibly affected (Fig. 17D2-ABZ-SO DHA ME, D3-blank DHA ME). Albendazole sulphoxide interacts with b-tubulin affecting the cytoskeletal structure required for maintaining the dynamics of vesicular traffic, and this action produces a vacuolation in the tegumental layer. Degenerative changes in cysts with blank DHA ME are attributed to ALP inhibition.

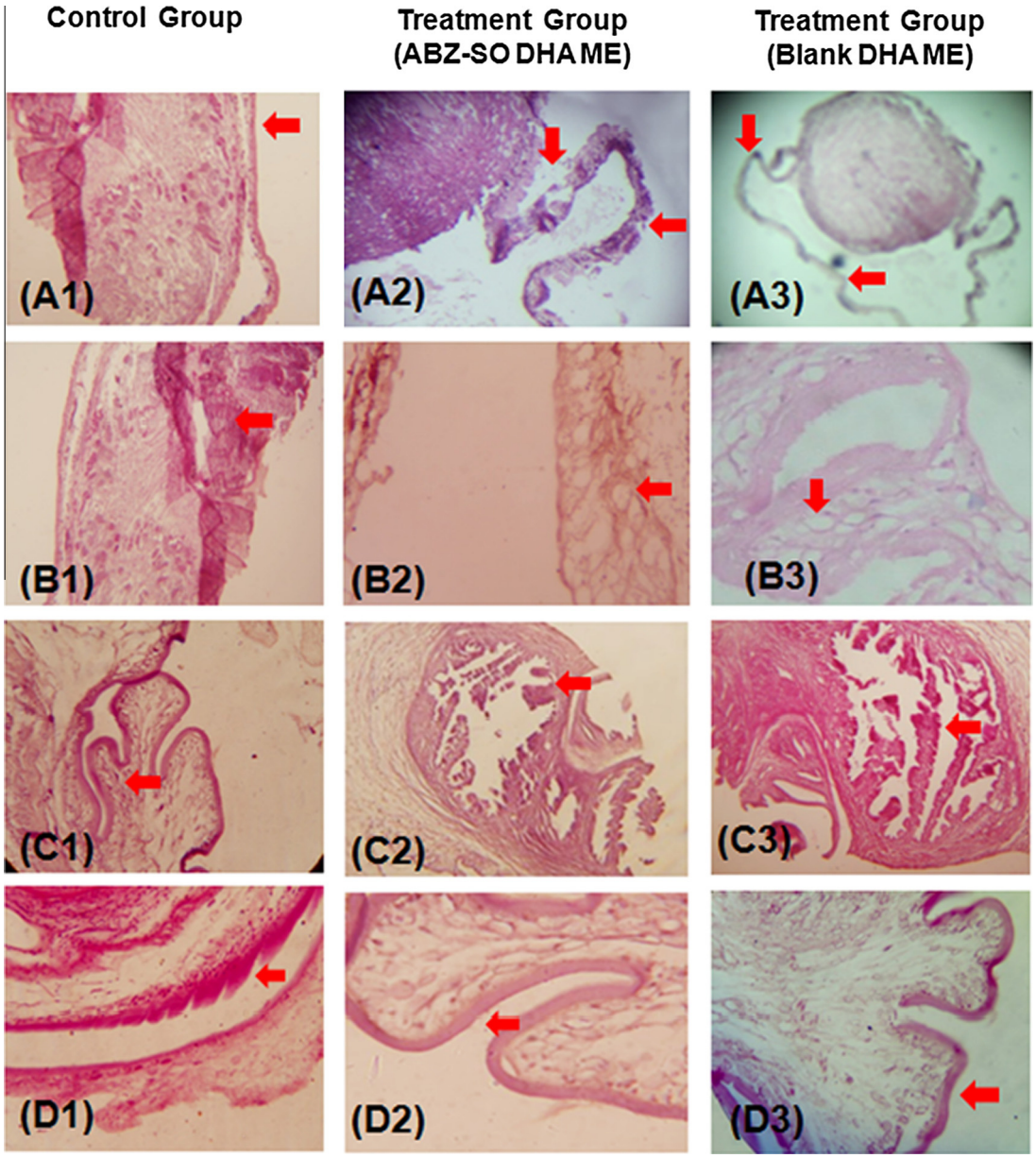

Fig. 17. Histopathology of *T. solium* cysts by light microscopy after 96 h of in vitro treatment. A1, B1, C1, and D1 represent control group, A2, B2, C2, and D2 represent treatment group (ABZ-SO DHA ME), A3, B3, C3, D3 represents treatment group (DHA ME). A1 intact cell wall, A2 and A3 disintegrated cell wall, B1 compact parenchyama, B2 and B3 vacuolization, C1 intact tegumental wall, C2 and C3 disintegrated tegumental wall, D1 presence of microtriches, D2 and D3 absence of microtriches.

4. Conclusion

Our study reports for the first time this novel combination of ABZ-SO and CUR for improved therapy of NCC. It is evident that while the MEs provide advantage for targeted delivery to the brain, the DHA ME provides an even greater benefit, confirming that DHA in the MEs plays crucial role not only in enhancing nose to brain delivery, but also in maintaining sustained level up to 24 h and also for its possible role in enhancing efficacy. The DHA ME proves to be a superior intranasal delivery system for targeted nose to brain delivery.

Conflict of interest

The authors report no conflict of interest.

Acknowledgement

Authors are thankful to University Grant Commission, Government of India for providing fellowship to Rajshree.

Appendix A. Supplementary material

Supplementary data associated with this article can be found, in the online version, at http://dx.doi.org/10.1016/j.ejpb.2015.08.008.

References

[1] L. Illum, Nasal drug delivery: problems, possibilities and solutions, J. Control. Rel. 87 (2003) 187–198, http://dx.doi.org/10.1016/S0168-3659(02)00363-2.
[2] H.R. Costantino, L. Illum, G. Brandt, P.H. Johnson, S.C. Quay, Intranasal delivery: physicochemical and therapeutic aspects, Int. J. Pharm. 337 (2007) 1–24, http://dx.doi.org/10.1016/j.ijpharm.2007.03.025.

[3] P.V. Devarajan, R.L. Shinde, Advances in microemulsions and nanoemulsions for improved therapy in brain cancer, in: E. Souto (Ed.), Advanced Anticancer Approaches with Multifunctional Lipid Nanocarriers, i Smithers – Creative Publishing Solutions, UK, 2011, pp. 347–394.
[4] J. Piazza, T. Hoare, L. Molinaro, K. Terpstra, J. Bhandari, P.R. Selvaganapathy, B. Gupta, R.K. Mishra, Haloperidol-loaded intranasally administered lectin functionalized poly (ethylene glycol)–block-poly (D,L)-lactic-co-glycolic acid (PEG–PLGA) nanoparticles for the treatment of schizophrenia, Eur. J. Pharm. Biopharm. 87 (2014) 30–39, http://dx.doi.org/10.1016/j.ejpb.2014.02.007.
[5] V.V. Jogani, P.J. Shah, P. Mishra, A.K. Mishra, A.R. Misra, Intranasal mucoadhesive microemulsion of tacrine to improve brain targeting, Alzheimer Dis. Assoc. Disord. 22 (2008) 116–124, http://dx.doi.org/10.1097/WAD.0b013e318157205b.
[6] Y.H. Lee, K.H. Kim, I.K. Yoon, K.E. Lee, I.K. Chun, J.Y. Rhie, H.S. Gwak, Pharmacokinetic evaluation of formulated levodopa methyl ester nasal delivery systems, Eur. J. Drug Metabo. Pharmacokinet. 39 (2014) 237–242, http://dx.doi.org/10.1007/s13318-013-0171-8.
[7] E. Gavini, G. Rassu, L. Ferraro, S. Beggiato, A. Alhalaweh, S. Velaga, N. Marchetti, P. Bandiera, P. Giunchedi, A. Dalpiaz, Influence of polymeric microcarriers on the in vivo intranasal uptake of an anti-migraine drug for brain targeting, Eur. J. Pharm. Biopharm. 83 (2013) 174–183, http://dx.doi.org/10.1016/j.ejpb.2012.10.010.
[8] X. Zhuang, X. Xiang, W. Grizzle, D. Sun, S. Zhang, R.C. Axtell, S. Ju, J. Mu, L. Zhang, L. Steinman, D. Miller, H.G. Zhang, Treatment of brain inflammatory diseases by delivering exosome encapsulated anti-inflammatory drugs from the nasal region to the brain, Mol. Ther. 19 (2011) 1769–1779, http://dx.doi.org/10.1038/mt.2011.164.
[9] T.E. Nash, G. Singh, A.C. White, V. Rajshekhar, J.A. Loeb, J.V. Proano, O.M. Takayanagui, A.E. Gonzalez, J.A. Butman, C. DeGiorgio, O.H. Del Brutto, A. Delgado-Escueta, C.A.W. Evans, R.H. Gilman, S.M. Martinez, M.T. Medina, E.J. Pretell, J. Teale, H.H. Garcia, Treatment of neurocysticercosis current status and future research needs, Neurology 67 (2006) 1120–1127, http://dx.doi.org/10.1212/01.wnl.0000238514.51747.3a.
[10] K.E. Mwape, I.K. Phiri, N. Praet, N. Speybroeck, J.B. Muma, P. Dorny, S. Gabriël, The incidence of human cysticercosis in a rural community of Eastern Zambia, PLoS Negl. Trop. Dis. 7 (2013) e2142, http://dx.doi.org/10.1371/journal.pntd.0002142.
[11] S. Mahanty, A. Paredes, M. Marzal, E. Gonzalez, S. Rodriguez, P. Dorny, C. Guerra-Giraldez, H.H. Garcia, T. Nash, Sensitive in vitro system to assess morphological and biochemical effects of praziquantel and albendazole on Taenia solium cysts, Antimicrob. Agents Chemother. 55 (2011) 211–217, http://dx.doi.org/10.1128/AAC.00761-10.
[12] F. Palomares, G. Palencia, J.R. Ambrosio, A. Ortiz, H. Jung-Cook, Evaluation of the efficacy of albendazole sulphoxide and praziquantel in combination on Taenia crassiceps cysts: in vitro studies, J. Antimicrob. Chemother. 57 (2006) 482–488, http://dx.doi.org/10.1093/jac/dki484.
[13] P. Venkatesan, Albendazole, J. Antimicrob. Chemother. 41 (1998) 145–147, http://dx.doi.org/10.1093/jac/41.2.145.
[14] M.J. Lawrence, G.D. Rees, Microemulsion-based media as novel drug delivery systems, Adv. Drug Deliv. Rev. 45 (2000) 89–121, http://dx.doi.org/10.1016/S0169-409X(00)00103-4.
[15] R.L. Shinde, A.B. Jindal, P.V. Devarajan, Microemulsions and nanoemulsions for targeted drug delivery to the brain, Curr. Nanosci. 7 (2011) 119–133, http://dx.doi.org/10.2174/157341311794480282.
[16] T.K. Vyas, A.K. Babbar, R.K. Sharma, S. Singh, A. Misra, Preliminary brain-targeting studies on intranasal mucoadhesive microemulsions of sumatriptan, AAPS PharmSciTech. 7 (2006) E49–E57, http://dx.doi.org/10.1208/pt070108.
[17] T.K. Vyas, A.K. Babbar, R.K. Sharma, S. Singh, A. Misra, Intranasal mucoadhesive microemulsions of clonazepam: preliminary studies on brain targeting, J. Pharm. Sci. 95 (2006) 570–580, http://dx.doi.org/10.1002/jps.20480.
[18] M. Kumar, A. Misra, A.K. Mishra, P. Mishra, K. Pathak, Mucoadhesive nanoemulsion-based intranasal drug delivery system of olanzapine for brain targeting, J. Drug Target. 16 (2008) 806–814, http://dx.doi.org/10.1080/10611860802476504.
[19] M. Kumar, A. Misra, A.K. Babbar, A.K. Mishra, P. Mishra, K. Pathak, Intranasal nanoemulsion based brain targeting drug delivery system of risperidone, Int. J. Pharm. 358 (2008) 285–291, http://dx.doi.org/10.1016/j.ijpharm.2008.03.029.
[20] T.K. Vyas, A.K. Babbar, R.K. Sharma, A. Misra, Intranasal mucoadhesive microemulsions of zolmitriptan: preliminary studies on brain-targeting, J. Drug Target. 13 (2005) 317–324, http://dx.doi.org/10.1080/10611860500246217.
[21] Q. Zhang, X. Jiang, W. Jiang, W. Lu, L. Su, Z. Shi, Preparation of nimodipine-loaded microemulsion for intranasal delivery and evaluation on the targeting efficiency to the brain, Int. J. Pharm. 275 (2004) 85–96, http://dx.doi.org/10.1016/j.ijpharm.2004.01.039.
[22] T.K. Vyas, A. Shahiwala, M.M. Amiji, Improved oral bioavailability and brain transport of Saquinavir upon administration in novel nanoemulsion formulations, Int. J. Pharm. 347 (2008) 93–101, http://dx.doi.org/10.1016/j.ijpharm.2007.06.016.
[23] W.J. Lukiw, N.G. Bazan, Docosahexaenoic acid and the aging brain, J. Nutr. 138 (2008) 2510–2514, http://dx.doi.org/10.3945/jn.108.096016.
[24] G. Virkel, A. Lifschitz, J. Sallovitz, A. Pis, C. Lanusse, Comparative hepatic and extrahepatic enantioselective sulfoxidation of albendazole and fenbendazole in sheep and cattle, Drug Metab. Dispos. 32 (2004) 536–544, http://dx.doi.org/10.1124/dmd.32.5.536.
[25] N. Chainani-Wu, Safety and anti-inflammatory activity of curcumin: a component of tumeric (Curcuma longa), J. Altern. Complement. Med. 9 (2003) 161–168, http://dx.doi.org/10.1089/107555303321223035.
[26] M.J. Patel, N.M. Patel, R.B. Patel, R.P. Patel, Formulation and evaluation of self-microemulsifying drug delivery system of lovastatin, Asian J. Pharm. Sci. 5 (2010) 266–275.
[27] S. Setthacheewakul, S. Mahattanadul, N. Phadoongsombut, W. Pichayakorn, R. Wiwattanapatapee, Development and evaluation of self-microemulsifying liquid and pellet formulations of curcumin, and absorption studies in rats, Eur. J. Pharm. Biopham. 76 (2010) 475–485, http://dx.doi.org/10.1016/j.ejpb.2010.07.011.
[28] R. Jain, S. Nabar, P. Dandekar, P. Hassan, V. Aswal, Y. Talmon, T. Shet, L. Borde, K. Ray, V. Patravale, Formulation and evaluation of novel micellar nanocarrier for nasal delivery of sumatriptan, Nanomedicine 5 (2010) 575–587, http://dx.doi.org/10.2217/nnm.10.28.
[29] M.J. Pastoriza-Gallego, L. Lugo, J.L. Legido, M.M. Piñeiro, Rheological non-Newtonian behaviour of ethylene glycol-based Fe_2O_3 nanofluids, Nanoscale Res. Lett. 6 (2011) 1–7, http://dx.doi.org/10.1186/1556-276X-6-560.
[30] N. Thirawong, J. Nunthanid, S. Puttipipatkhachorn, P. Sriamornsak, Mucoadhesive properties of various pectins on gastrointestinal mucosa: an in vitro evaluation using texture analyzer, Eur. J. Pharm. Biopharm. 67 (2007) 132–140, http://dx.doi.org/10.1016/j.ejpb.2007.01.010.
[31] T.K. Bock, B.W. Müller, A novel assay to determine the hemolytic activity of drugs incorporated in colloidal carrier systems, Pharm. Res. 11 (1994) 589–591, http://dx.doi.org/10.1023/A:1018987120738.
[32] H.D. Han, B.C. Shin, H.S. Choi, Doxorubicin-encapsulated thermosensitive liposomes modified with poly (N-isopropylacrylamide-co-acrylamide): drug release behavior and stability in the presence of serum, Eur. J. Pharm. Biopharm. 62 (2006) 110–116, http://dx.doi.org/10.1016/j.ejpb.2005.07.006.
[33] H.S. Mahajan, V.K. Tyagi, R.R. Patil, S.B. Dusunge, Thiolated xyloglucan: synthesis, characterization and evaluation as mucoadhesive in situ gelling agent, Carbohydr. Polym. 91 (2013) 618–625, http://dx.doi.org/10.1016/j.carbpol.2012.08.077.
[34] L. Kozlovskaya, M. Abou-Kaoud, D. Stepensky, Quantitative analysis of drug delivery to the brain via nasal route, J. Control. Rel. 189 (2014) 133–140, http://dx.doi.org/10.1016/j.jconrel.2014.06.053.
[35] Z. Dong, H. Katsumi, T. Sakane, A. Yamamoto, Effects of polyamidoamine (PAMAM) dendrimers on the nasal absorption of poorly absorbable drugs in rats, Int. J. Pharm. 393 (2010) 245–253, http://dx.doi.org/10.1016/j.ijpharm.2010.04.021.
[36] D. Dunston, S. Ashby, K. Krosnowski, T. Ogura, W. Lin, An effective manual deboning method to prepare intact mouse nasal tissue with preserved anatomical organization, J. Vis. Exp. 78 (2013) 10, http://dx.doi.org/10.3791/50538.
[37] C.L. Saw, Y. Huang, A.N. Kong, Synergistic anti-inflammatory effects of low doses of curcumin in combination with polyunsaturated fatty acids: docosahexaenoic acid or eicosapentaenoic acid, Biochem. Pharmacol. 79 (2010) 421–430, http://dx.doi.org/10.1016/j.bcp.2009.08.030.
[38] G. Corace, C. Angeloni, M. Malaguti, S. Hrelia, P.C. Stein, M. Brandl, R. Gotti, B. Luppi, Multifunctional liposomes for nasal delivery of the anti-Alzheimer drug tacrine hydrochloride, J. Liposome Res. 24 (2014) 323–335, http://dx.doi.org/10.3109/08982104.2014.899369.
[39] K. Dae-Duk, In vitro cellular models for nasal drug absorption studies, in: E. Carsten, K. Kwang-Jin (Eds.), Drug Absorption Studies: In Situ, In Vitro and In Silico Models, Springer, USA, 2007, pp. 216–234, http://dx.doi.org/10.1007/978-0-387-74901-3_9.
[40] M.A. Dobrovolskaia, J.D. Clogston, B.D. Neun, J.B. Hall, A.K. Patri, S.E. McNeil, Method for analysis of nanoparticle hemolytic properties in vitro, Nano Lett. 8 (2008) 2180–2187, http://dx.doi.org/10.1021/nl0805615.
[41] Z. Hossain, H. Kurihara, M. Hosokawa, K. Takahashi, Docosahexaenoic acid and eicosapentaenoic acid-enriched phosphatidylcholine liposomes enhance the permeability, transportation and uptake of phospholipids in Caco-2 cells, Mol. Cell. Biochem. 285 (2006) 155–163, http://dx.doi.org/10.1007/s-11010-005-9074-6.
[42] M. Usami, T. Komurasaki, A. Hanada, K. Kinoshita, A. Ohata, Effect of γ-linolenic acid or docosahexaenoic acid on tight junction permeability in intestinal monolayer cells and their mechanism by protein kinase C activation and/or eicosanoid formation, Nutrition 19 (2003) 150–156, http://dx.doi.org/10.1016/S0899-9007(02)00927-9.
[43] S. Roig-Pérez, N. Cortadellas, M. Moretó, R. Ferrer, Intracellular mechanisms involved in docosahexaenoic acid-induced increases in tight junction permeability in Caco-2 cell monolayers, J. Nutr. 140 (2010) 1557–1563, http://dx.doi.org/10.3945/jn.109.120469.
[44] F. Buyukozturk, J.C. Benneyan, R.L. Carrier, Impact of emulsion-based drug delivery systems on intestinal permeability and drug release kinetics, J. Control. Rel. 142 (2010) 22–30, http://dx.doi.org/10.1016/j.jconrel.2009.10.005.
[45] R.A. Siddiqui, K. Harvey, E. Bammerlin, N. Ikhlaque, Docosahexaenoic acid: a potential modulator of brain tumors and metastasis, J. Biomol. Res. Ther. 2 (2013) 3, http://dx.doi.org/10.4172/2167-7956.1000e119.
[46] M. Picq, P. Chen, M. Perez, M. Michaud, E. Véricel, M. Guichardant, M. Lagarde, D.H.A. Metabolism, Targeting the brain and lipoxygenation, Mol. Neurobiol. 42 (2010) 48–51, http://dx.doi.org/10.1007/s12035-010-8131-7.

[47] S. Tamilvanan, Formulation of multifunctional oil-in-water nanosized emulsions for active and passive targeting of drugs to otherwise inaccessible internal organs of the human body, Int. J. Pharm. 381 (2009) 62–76, http://dx.doi.org/10.1016/j.ijpharm.2009.08.001.

[48] L.N. Nguyen, D. Ma, G. Shui, P. Wong, A. Cazenave-Gassiot, X. Zhang, M.R. Wenk, E.L. Goh, D.L. Silver, Mfsd2a is a transporter for the essential omega-3 fatty acid docosahexaenoic acid, Nature 509 (2014) 503–506, http://dx.doi.org/10.1038/nature13241.

[49] J. Kreuter, D. Shamenkov, V. Petrov, P. Ramge, K. Cychutek, C. Koch-Brandt, R. Alyautdin, Apolipoprotein-mediated transport of nanoparticle-bound drugs across the blood-brain barrier, J. Drug Target. 10 (2002) 317–325, http://dx.doi.org/10.1080/10611860290031877.

[50] J. Kreuter, P. Ramge, V. Petrov, S. Hamm, S.E. Gelprina, B. Engelhardt, R. Alyautdin, H. von Briesen, D.J. Begley, Direct evidence that polysorbate-80-coated poly(butyl cyanoacrylate) nanoparticles deliver drugs to the CNS via specific mechanisms requiring prior binding of the drug to the nanoparticles, Pharm. Res. 20 (2003) 409–416.

[51] T.M. Goppert, R.H. Müller, Polysorbate-stabilized solid lipid nanoparticles as colloidal carriers for intravenous targeting of drugs to the brain: comparison of plasma protein adsorption patterns, J. Drug Target. 13 (2005) 179–187, http://dx.doi.org/10.1080/10611860500071292.

[52] A. Swargiary, B. Roy, B. Ronghang, B., Partial characterisation of alkaline phosphatase in Fasciolopsis buski – an intestinal fluke treated with crude extract of Alpinia nigra (Zingiberaceae), J. Pharm. Technol. Drug Res. 2 (2013) 5, http://dx.doi.org/10.7243/2050-120X-2-5.

[53] M. Coetzee, M. Haag, M.C. Kruger, Effects of arachidonic acid and docosahexaenoic acid on differentiation and mineralization of MC3T3-E1 osteoblast-like cells, Cell Biochem. Funct. 27 (2009) 3–11, http://dx.doi.org/10.1002/cbf.1526.